DYNAMIC MODELLING AND ANALYSIS OF SHAFT WITH ROTOR SUPPORTED ON BALL BEARING HAVING SQUEEZE FILM DAMPER

A THESIS SUBMITTED IN PARTIAL FULFILLMENT OF THE REQUIREMENT
FOR THE AWARD OF THE DEGREE OF

MASTER OF TECHNOLOGY

(COMPUTATIONAL DESIGN)

TO

DELHI TECHNOLOGICAL UNIVERSITY

SUBMITTED BY

PUSHPENDRA KUMAR YADAV

ROLL NO.:2K15/CDN/12

UNDER THE GUIDANCE OF

DR. VIKAS RASTOGI

PROFESSOR

DELHI TECHNOLOGICAL UNIVERSITY

DEPARTMENT OF MECHANICAL ENGINEERING

DELHI TECHNOLOGICAL UNIVERSITY

BAWANA ROAD, DELHI-110042

DELHI TECHNOLOGICAL UNIVERSITY

(Formerly Delhi college of Engineering)

Shahbad Daulatpur, Bawana Road,

Delhi-110042

STUDENT'S DECLARATION

I, **PUSHPENDRA KUMAR YADAV,** hereby certify that the work which is being presented in this thesis entitled **"Dynamic Modelling and Analysis of shaft with rotor supported on ball bearing having squeeze film damper"** is submitted in the partial fulfilment of the requirement for degree of **Master of Technology (Computational Design)** in Department of Mechanical Engineering at **Delhi Technological University** is an authentic record of my own work carried out under the supervision of **Prof. Vikas Rastogi.** The matter presented in this thesis has not been submitted in any other University/Institute for the award of Master of Technology Degree. Also, it has not been directly copied from any source without giving its proper reference.

Signature of Student

This is to certify that the above statement made by the candidate is correct to the best of my knowledge.

Signature of Supervisor

DELHI TECHNOLOGICAL UNIVERSITY

(Formerly Delhi college of Engineering)

Shahbad Daulatpur, Baawana Road,

Delhi-110042

CERTIFICATE

This is to certify that this thesis report entitled, **"Dynamic Modelling and Analysis f shaft with rotor supported on ball bearing having squeeze film damper "** being submitted by **Pushpendra kumar yadav (Roll No. 2K15/CDN/12)** at Delhi Technological University, Delhi for the award of the Degree of Master of Technology as per academic curriculum. It is a record of bonafide research work carried out by the student under my supervision and guidance, towards partial fulfilment of the requirement for the award of Master of Technology degree in Computational Design. The work is original as it has not been submitted earlier in part or full for any purpose before.

Dr. Vikas Rastogi

Professor

Mechanical Engineering Department

Delhi Technological University

Delhi-110042

ACKNOWLEDGEMENT

PUSHPENDRA KUMAR YADAV

M.Tech (COMPUTATIONAL DESIGN)

2K15/CDN/12

ABSTRACT

The dynamics of turbo machinery depends upon the behaviour of the rotor, which is strongly affected by the rotor's supports. The bearings supporting the rotor generally have very less damping, which can sometimes leads to very large vibration amplitude of rotor when it is operated near its operating range. Squeeze film damper is one of the most widely used tools to provide an additional external damping for rotating equipments. So, to reduce the vibration amplitude of rotor squeeze film damper can be used.

Presently, this work is dedicated to analyse the dynamic behaviour of shaft with rotor supported on ball bearing having squeeze film damper with the help of bond graph technique. First, physical and mathematical model of various element of rig such as squeeze film damper having centralizing spring, rigid rotor on shaft and bearing support has been prepared. The bond graph modelling of shaft, spinning hub, squeeze film damper is done using symbol sonata software bond pad. Simulation of this model has been carried out on Symbols sonata software which uses the fourth order Runge-Kutta method. The variation in the position of centre mass of rotor with change in various parameters such as speed, clearance, viscosity of oil and stiffness of centralizing spring is observed. The data obtained is used to get plots .

Keywords: Bond graph modelling, Damper , Squeeze film damper, Rotor Dynamics, Vibration analysis, Ball bearing , Bearing support .

TABLE OF CONTENTS

CHAPTER 1: INTRODUCTION

LIST OF FIGURES

CHAPTER 1 : INTRODUCTION

CHAPTER 3 : MATHEMATICAL MODELLING

CHAPTER 4 : BOND GRAPH MODELLING

Chapter 5 : Simulation Study

CHAPTER 6 : RESULTS AND DISCUSSION

LIST OF TABLES

CHAPTER 4 : BOND GRAPH MODELLING

CHAPTER -5 : SIMULATION STUDY

CHAPTER 1

INTRODUCTION

1.1 Introduction

In this chapter, the general comprehensive description of ball bearing with squeeze film damper is presented. The objectives are stated and an overview of the organization of the rest of the thesis is described.

1.2 Significance of the study of rotating shaft with squeeze film damper

Today, many researchers are widely focused on the design of rotating machines to enhance the performance and stability of rotating machines and improving them to provide more space for other components of rotor such as disks, impellers, and blades. Among the various elements of the rotating machine, the shaft of rotors plays a crucial role to get a high level of rotational energy and increase the power generated.

In addition, shaft is a important element of future high speed rotating machines so efforts are done to decrease unwanted vibrations. Increasing the damping of the system is considered as one of the most common solutions for the reduction in unwanted vibrations of the rotor. In this type of applications, it is necessary to have a moderate amount of damping in the system to traverse the critical speeds with low amplitude of motion and to maintain the rotor system stable. Squeeze film damper is one of the most widely used tools to provide an additional external damping for rotating equipments.

1.2.1 Importance of damper in Turbomachinary

The dynamics of turbo machinery depends upon the behavior of the rotor, which is strongly affected by the rotor's supports. Designing the shaft supports for high speed turbines is a difficult task; the design of the shafts supports for aviation jet engines must also address additional requirements coming from safety regulations that actually make ball bearings compulsory, thus designers must use added devices to tune the stiffness and damping of the shaft supports to obtain correct shaft dynamics. It is also very mostly known that rotating shafts in turbines and

generators are prone to vibrations and dynamic loads caused by rotor or shaft imbalances. Most types of bearings in such systems, however provide very minute damping to the system. In applications of this type, it is necessary to have a moderate amount of damping in the system to traverse the critical speeds .With low amplitude of motion and to maintain the rotor system stable. That is, in a system which has negligible damping, such as a system having ball bearings, the system passes one or more resonant frequencies as the system moves toward its operating speed. The vibrations can be so large that they can hinder working of the machine and the high amplitude of vibration can result in failure of the component. So damping of the system is required during startup and shutdown to avoid adverse effects on the system at resonant frequencies.

1.2.2 Various types of bearing systems

The standard definition of a bearing is a device or system which can transmit a load through two elements of the system moving relatively to each other. The other requirement is to allow relative movement with minimum amount of power being used. There are many ways of achieving this. Some of them are explained below:

1.2.2.1 Rolling element bearing

A rolling-element bearing, also known as a rolling bearing, is a bearing which carries a load by placing rolling elements (such as balls or rollers) between two bearing rings called races. The relative motion of the races causes the rolling elements to roll with very little rolling resistance and with little sliding.

Rolling-element bearing has the benefit of a good transaction between cost, size, weight, carrying capacity, durability, accuracy, friction, and so on. Other bearing designs are frequently better on one exact attribute, but not good in generally other attributes. There are five type of rolling elements that are used in rolling-element bearings: balls, cylindrical rollers, spherical rollers, tapered rollers, and needle rollers. Most rolling-element bearings features cage. The cages lessen friction, wear and prevent the elements from rubbing against each other. Typical rolling-element bearings size ranges from 10 mm diameter to a few metres

diameter, and have load-carrying capacity from a few tens of grams to many thousands of tonnes.

1.2.2.1.1 Ball bearing

A most common type of rolling-element bearing is the ball bearing. The bearing has inner and outer races between which ball rolls. Each race has a groove usually shaped so the ball fits a little loose. Thus, in principle, the ball contacts each race across a very narrow area. However, a load on an infinitely small point would cause infinitely high contact pressure.. Thus, the contact between ball and race is of finite size and has finite pressure. Note also that the deformed ball and race do not roll entirely smoothly because different parts of the ball are moving at different speeds as it rolls. Thus, there are opposing forces and sliding motions at each ball/race contact.
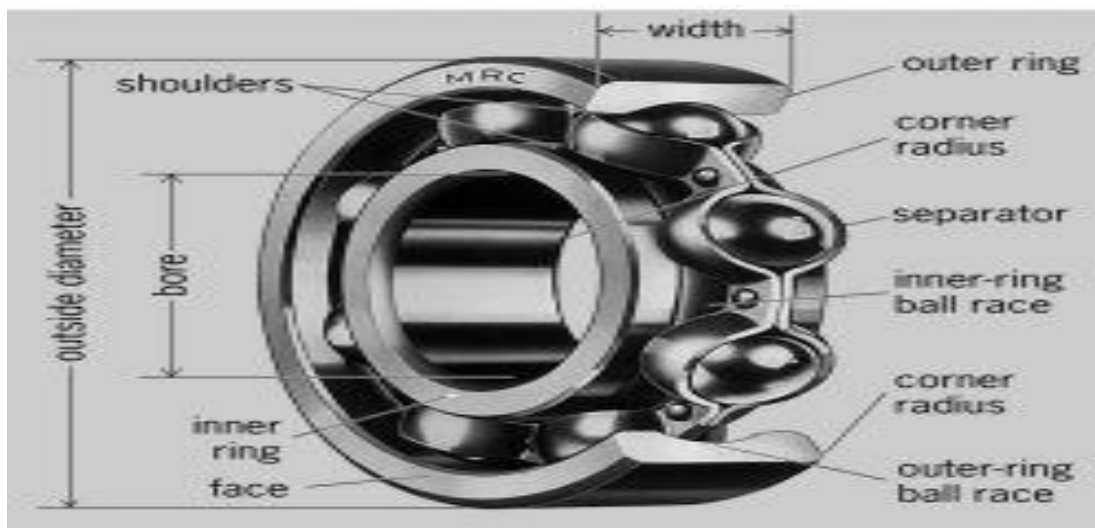
Figure 1.1: Ball bearing [22]

1.2.2.1.2 Roller bearing

Roller bearings typically have higher radial load capacity than ball bearings, but a lower capacity and higher friction under axial loads. If the inner and outer races are misaligned, the bearing capacity often drops quickly compared to either a ball bearing.

Roller bearing can be classified into following types:

1. **Cylindrical roller**: Common roller bearings use cylinders of slightly greater length than diameter.
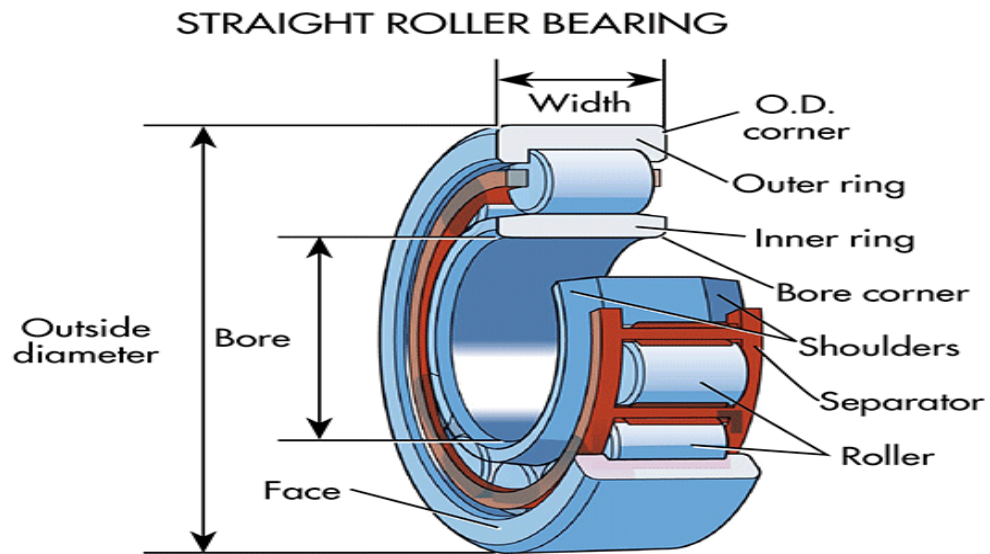
Figure 1.2: Cylindrical Roller Bearing[23]

2. Spherical roller bearing :

Spherical roller bearings have an outer ring with an internal spherical shape. The rollers are thicker in the middle and thinner at the ends. Spherical roller bearings can thus accommodate both static and dynamic misalignment.
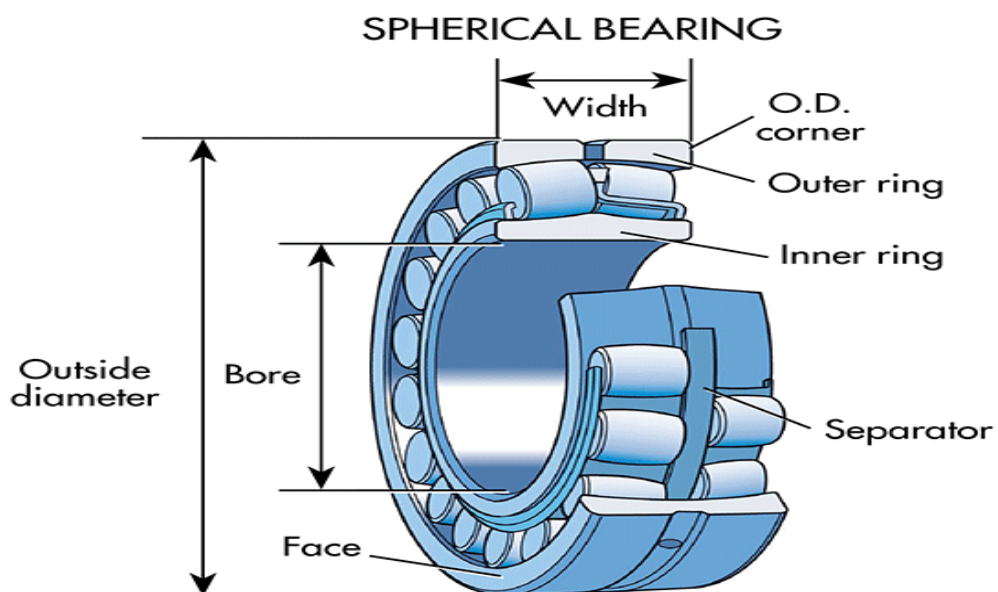
Figure 1.3: Spherical Roller bearing[23]

3. Gear bearing

Gear bearing is roller bearing combining to epicyclical gear. Each element of it is represented by concentric alternation of rollers and gearwheels with equality of roller(s) diameter(s) to gearwheel(s) pitch diameter(s). The widths of conjugated rollers and gearwheels in pairs are the same.

4. Tapered roller

Tapered roller bearings use conical rollers that run on conical races. Most roller bearings only take radial or axial loads, but tapered roller bearings support both radial and axial loads, and generally can carry higher loads than ball bearings due to greater contact area.
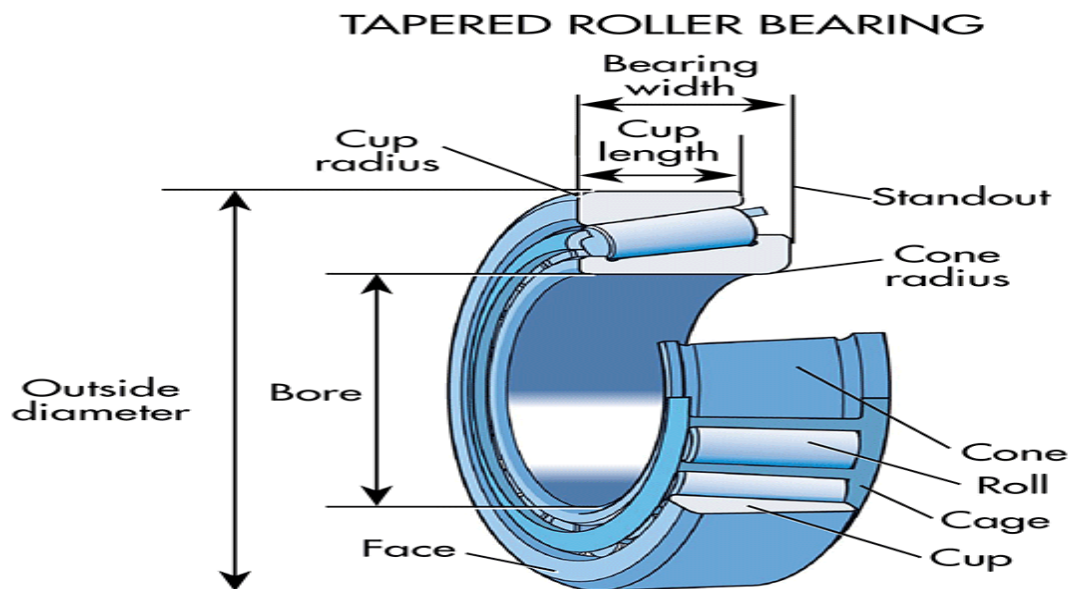
Figure 1.4 : Tapered Roller bearing[23]

]

5. Needle roller bearings

Needle roller bearings use very long and thin cylinders. Often the ends of the rollers taper to points, and these are used to keep the rollers captive, or they may be hemispherical and not captive but held by the shaft itself or a similar arrangement. Since the rollers are thin, the outside diameter of the bearing is only slightly larger

than the hole in the middle. However, the small-diameter rollers must bend sharply where they contact the races, and thus the bearing fatigues relatively quickly.
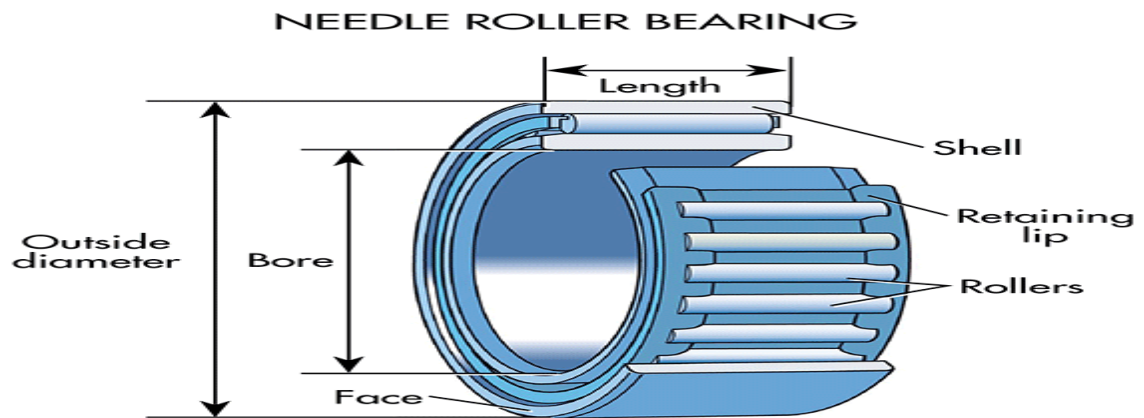
Figure 1.5 : Needle roller bearings[23]

`1.2.2.2 Air Bearing:

Air bearing are bearings that use a thin film of pressurized air to provide an exceedingly low friction load-bearing interface between surfaces. The two surfaces do not touch. As they are contact-free, air bearings avoid the traditional bearing-related problems of friction, wear, particulates, and lubricant handling, and offer distinct advantages in precision positioning, such as lacking backlash and static friction, as well as in high-speed applications.

The fluid film of the bearing is air that flows through the bearing itself to the bearing surface. The design of the air bearing is such that, although the air constantly escapes from the bearing gap, the pressure between the faces of the bearing is enough to support the working loads

1.2.2.3 Plain bearing

A plain bearing (in railroading sometimes called a solid bearing) is the simplest type of bearing, comprising just a bearing surface and no rolling elements. Therefore, the journal (i.e., the part of the shaft in contact with the bearing) slides over the bearing surface. The simplest example of a plain bearing is a shaft rotating in a hole. A simple linear bearing can be a pair of flat surfaces designed to allow motion; e.g., a drawer and the slides it rests on[1] or the ways on the bed of a lathe.

Plain bearings, in general, are the least expensive type of bearing. They are also compact and lightweight, and they have a high load-carrying capacity. Plain bearings must be made from a material that is durable, low friction, low wear to the bearing and shaft, resistant to elevated temperatures, and corrosion resistant.

1.2.2.4 Hydrodynamic journal bearing

Hydrodynamic journal bearing is a bearing operating with hydrodynamic lubrication, in which the bearing surface is separated from the journal surface by the lubricant film generated by the journal rotation.
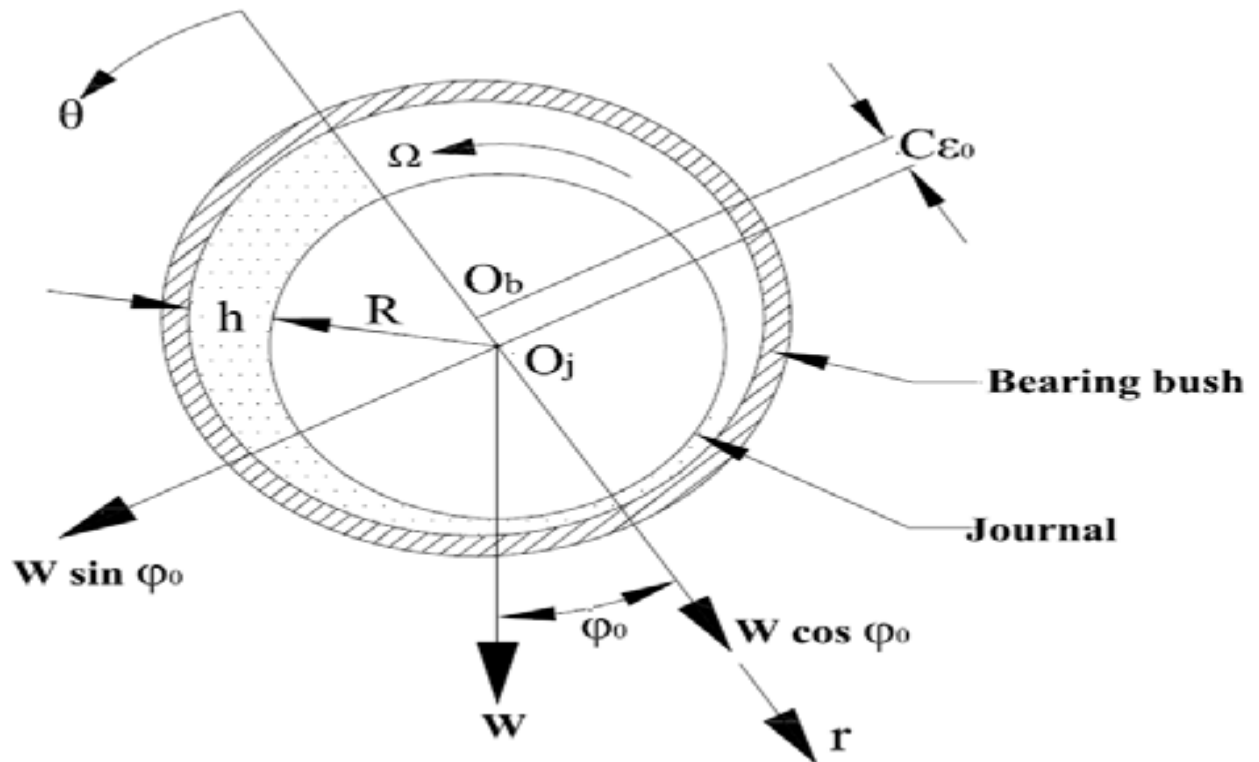
Figure 1.6: Hydrodynamic Journal Bearing[24]

The figure demonstrates a hydrodynamic journal bearing and a journal rotating in a clockwise direction. Journal rotation causes pumping of the lubricant (oil) flowing around the bearing in the rotation direction. If there is no force applied to the journal its position will remain concentric to the bearing position. However a loaded journal displaces from the concentric position and forms a converging gap between the bearing and journal surfaces. The pumping action of the journal forces the oil to squeeze through the wedge shaped gap generating a

7

pressure. The pressure falls to the cavitation pressure (close to the atmospheric pressure) in the diverging gap zone where cavitation forms.

Two types of cavitation may form in journal bearing:

- Gaseous cavitation associated with air and other gases dissolved in oil. If the oil pressure falls below the atmospheric pressure the gases tend to come out of the oil forming gaseous cavitation voids..
- Vapor cavitation forms when the load applied to the bearing fluctuates at high frequency (e.g. bearings in high RPM internal combustion engines). The oil pressure instantly falls causing formation of cavities due to fast evaporation (boiling).

The oil pressure creates a supporting force separating the journal from tbearing surface. The force of oil pressure and the hydrodynamic friction force counterbalance the external load F. The final position of the journal is determined by the equilibrium between the three forces.

1.2.2.5 Hydrostatic journal bearing

In a hydrostatic bearing an external source of pressurized fluid forces lubricant between two surfaces; thus enabling non-contacting operation and the ability to support a load. Hydrostatic bearings can support large loads without journal rotation and provide large (accurate and controllable) direct stiffness as well as damping (energy dissipation) coefficients.
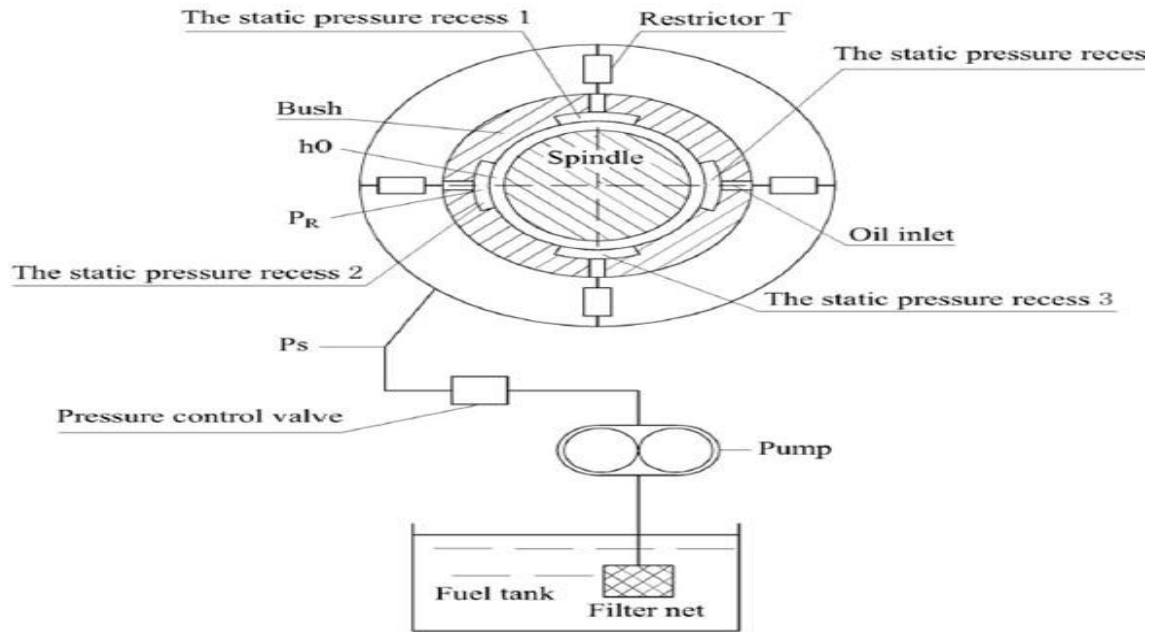
Figure 1.7: Hydrostatic journal bearing [25]

Hydrostatic bearings rely on external fluid pressurization to generate load support and a large centering stiffness, even in the absence of journal rotation. The load capacity and direct stiffness of hydrostatic bearings do not depend on fluid viscosity, thus making them ideal rotor support elements in process fluid pumps. Current applications intend to replace oil lubricated bearing with hybrid bearings to improve efficiency with shorten rotor spans and less mechanical complexity.

1.2.3 Squeeze-Film Dampers

Squeeze-film dampers can be regarded as a fluid-film cylindrical bearing without the rotation of the journal. The fluid film gets the shearing action due to the relative translatory motion of the bearing rather than the squeezing action due to the relative transverse motion of the damper . Squeeze-film dampers usage in attenuating vibrations is widespread in aircraft gas turbine industries as compared to the process industries where its preferred usage is as a band-aid solution without any preplanning. This is due to the reason that squeeze-film dampers are more complex to design than any other machine elements. The attenuation of sub harmonic rotor instabilities would be the main concern in the designer mind while designing a squeeze-film damper since steady state synchronous vibrations are relatively to tackle with modifications in the rotor and the bearing parameters itself.

Squeeze-film dampers can be used in both for rolling bearings and fluid-film bearings by providing arrangement for the squeezing of the film between the outer ring (or sleeve) and the housing, and the bearing bush (or sleeve) and the housing, respectively. The sleeve is slotted or pinned loosely to prevent its rotation. Since rolling bearings are extensively used in aircraft turbine engines and in such bearings the damping is very low. The squeeze-film damper is designed in series with rolling bearings provide enough damping to suppress unstable vibrations of the rotor system. Successful applications of such squeeze film mountings include the Rolls-Royce RB 203 and RB 211 and the Rover 2S/150R engines

The performance of squeeze-film dampers depends upon several geometrical, physical and operating parameters. Some of them are geometrical parameters: the length, the diameter, the radial clearance, the feed and discharge mechanisms, the type of seal ends; physical parameters: the viscosity of the lubricant; operating parameters: the lubricant supply pressure, the fluid inertia, and dynamic cavitations. Similar to bearings, the incompressible-fluid Reynolds equation is generally used to model the squeeze-film dampers. However, because of cavitation phenomena, the correlation between theory and experiment are in dampers is less as compared to bearings.

1.2.3.1 Design configuration of squeeze film damper with stiffed centralizing spring

The squeeze film damper is one of the most widely used tools to provide an additional external damping for rotating equipments. In its simplest form, the squeeze film damper consists of an oil filled annular cavity surrounding the outer race of a rolling element bearing. The outer race of the bearing, which acts as the journal of dampers, is prevented from rotating, but it is allowed to describe whirl motion around its equilibrium position. There are two types of configurations for the use of squeeze film dampers in rotating equipments: dampers with centralizing springs and those without centralizing springs. In the case of damper without centering spring, the journal that lies at the bottom of the clearance circle, is lifted when sufficient lift force is generated. In the case of damper with centralizing spring, the journal is constrained in the center of damper by a centralizing spring. The typical installation of both configurations is illustrated in Fig. 1.8.

10

.
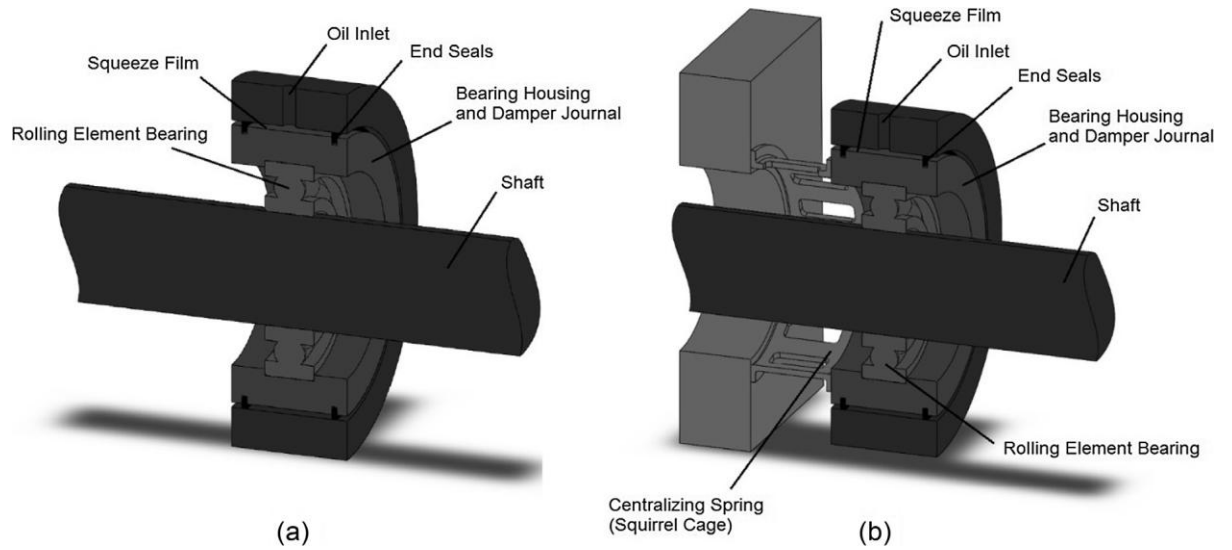
Figure 1.8. Two types of configuration for the use of squeeze film dampers in rotating equipments: (a) damper without centralizing spring and (b) damper with centralizing spring [21]

In our study we have considered a squeeze film damper with centralising spring as shown in below figure.
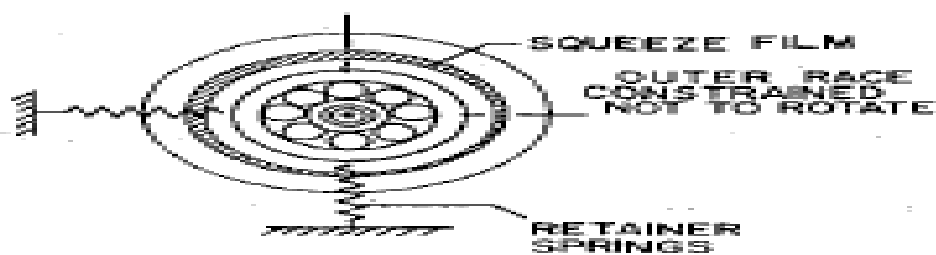
Figure 1.9 : Squeeze film damper with centralizing spring [3]

The configuration of a antifriction ball bearing with squeeze film damper having centralizing spring is shown in the above figure. It consist of a centrally mounted ball bearing having shaft inside it .The ball bearing is inside the journal of squeeze

film damper .The rotational motion of the squeeze film damper is constrained with the help of antifriction pin and centralizing spring which is mounted on a bearing support.

1.3 Modelling

Modelling is a process of producing model, whereas a model is representation of the working and construction of some system. Purpose of a model is to enable the analyst to predict the effect of changes to the system and it should be a close approximation to the real system and incorporate most of its salient features. Model should not be so complex that it is impossible to understand and experiment on it. A model is said to be good if it is judicious trade off between realism and simplicity. Model validity is an important issue in modelling. Validation techniques of model include simulating the model under known input conditions and comparing the output with the system output awesome experimental data available.

Most of the modern mechanical system form a part of multidisciplinary system and are closely coupled with the magnetic, hydraulic electrical or other kind of energy domains. Hierarchial approach is advantageous in modelling of an integrated dynamic system. Systematic approach minimises the modelling mistakes by breaking the system model into small components and subsystems, which are manageable in size and complexity. Same components can be used repeatedly without building blocks of the some part again. For example, an axle component in the Vehicle dynamics subsystem was built once and can be used for both rear and front axle. With hierarchial modelling, models of some component with different complexity can be easily be interchanged without changing the remaining structure of the model. The simulation process steps are shown in figure 1.10.
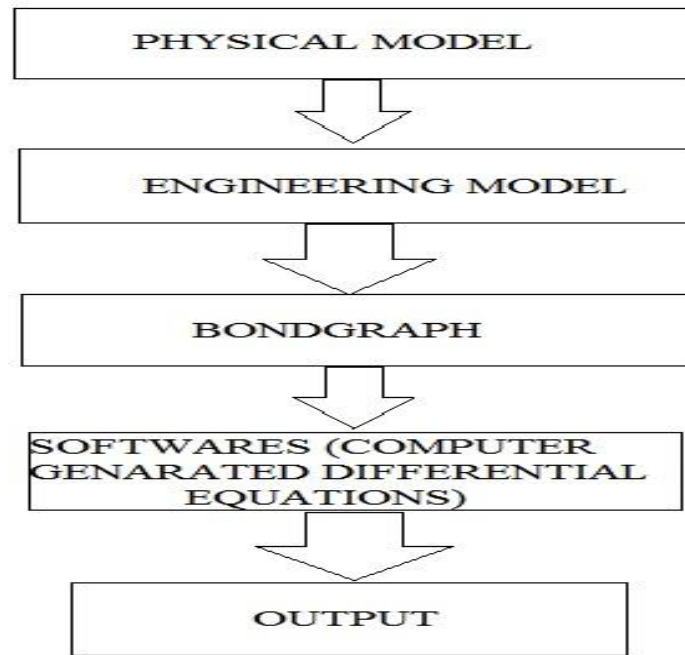
Figure 1.10 : Simulation process steps

The various approaches adopted in modelling of Rotor with squeeze film damper are stated as follows:

a) Ignoring body flexibility using a lumped mass model.
b) Modelling the shaft as a regular beam using Rayleigh beam model and calculating, measuring or estimating model masses and stiffness.
c) Modelling the mathematical model of different queeze film damper.
d) Modelling the dynamic behaviour of squeeze film damper using bond graph technique.

1.4 Significance of Bond graph modelling

In the 1950s H.M. Paynter of MIT worked on various interdisciplinary engineering projects including digital and analogue computing, hydroelectric plants, nonlinear dynamics and control. He observed that the similiar forms of equations were generated by dynamic system in a wide variety of domain (for example mechanical, fluid and electrical). He incorporated the notion of an energy port into his mythology and thus bond graph model was invented in 1959. Later Bond graph theory has been developed by many researchers.

Bond graph model is a is a graphical model approach of modelling, in which component energy parts are connected by bonds which supply the transfer of energy between the system components.

The bond graph language aspires to express general class of physical systems through the power interactions. Factor of power, i.e. Flow and Effort, have different interpretation in different physical domains. Hence power can be used as to generalized co-ordinate, to model coupled system residing in several energy domains in bond graph. One only needs to recognize for groups of basic symbols in bond graph , i.e., the three basic one port passive element inertance (I), Capacitance (C) Resistance (R) ; two basic active elements source of effort (SE) and source of flow (SF) ; two basic two port elements gyrator (GY) and transformer (TF) and two basic junctions i.e., constant flow junction(1) and constant effort junction (0). The basic variable of flow (f) , effort (e), the time integral of flow (Q) and the time integral of effort (P) . A physical system can be represented by lines and symbols, identifying the power flow by this approach . The lumped parameters element of inertance, capacitance and resistance are interconnected in the energy conserving way by junctions and bonds resulting in a network structure. The deviation of the system equation is so systematic that it can be algorithmzed from the pictorial representation of bond graph. Whole procedure of simulation and modelling of the system can be performed with some of the existing software example **Camp-G, ENPORT , 20sim, SYMBOL-shakti , COSMO** etc.

Main advantage of bond graph techniques are -

- Bond graphs can be used to describe simple linear and nonlinear systems.
- Bond graph provides a useful notion for the purpose of modelling physical systems.
- Systems with diverse energy domain are treated in and unified manner.
- Easiest way to communicate the description of energy flow in dynamic systems.
- By using power conservation properties of Bond graph may need to constraint velocities only and the forces will be automatically be balanced.

- Graphical representation of document complex models very easily and unambiguously.
- Model subsystems can be independently.

The present dissertation work explores the ability of bond graph to obtain dynamic behaviour and modelling of Rotor on squeeze film damper bearing based on physical paradigm of the system. Bond graph technique generally offers flexibility in modelling and formulation of system equations. A very large system may also be modelled in a modular forms by creating subsystem models and then joining them together at their interaction port to create an integrated system model. Modal is easy modified making it a powerful tool for system synthesis and consolidation of the innovative ideas. Bond graph equations normally used generalise displacement and generalized movement as state variables. The bond graph modelling, their simulation and animation is performed using SYMBOLS Sonata® a bond graph modelling software.

1.5 Research objective

The research's objective is:

- To create the dynamic model of squeeze film damper by using bond graph technique.
- To create it's mathematical model.
- To create the dynamic model of shaft and rotor by using bond graph technique.
- To create it's mathematical model .
- Simulation of the bond graph model of rotor with squeeze film damper bearing for variable parameters to obtain behaviour of rotor's centre of mass.

1.6 Organization of Thesis

The chapters of the thesis are arranged in the following manner. *Chapter 1* discusses about the Significance of the project along with describing different types of bearings and a brief description of the Squeeze film damper bearing configuration. The primary goal of this chapter is to provide the reader a rough

idea about this thesis. *Chapter 2* discusses some literature reviews. *Chapter 3* presents the mathematical modelling of SFD with centralizing spring , Rigid rotor and bearing support. *Chapter 4* presents the bond graph modelling of SFD , shaft etc. *Chapter 5* presents simulation study .*Chapter 6* deals with results and discussion. *Chapter 7* concludes the thesis and also suggest some score for future work.

CHAPTER -2

LITERATURE REVIEW

2.1 Introduction

In this chapter the background of various investigation and the literature review are briefly presented. There are various studies , which are contributed by researchers regarding the Squeeze film damper analysis , however very few researches are carried out analyzing behaviour of squeeze film damper by bond graph modelling .In this project the effect of change in various parameters of squeeze film damper is observed. Some research relating to squeeze film bearing and bond graph modelling are as follows.

2.2 LITERATURE REVIEW

Modaresahmadi et al.[1] presented a paper on dynamic analysis of a rotor supported on ball bearings with waviness and centralizing springs and squeeze film dampers. In this work presented that a crucial parameter associated with manufacturing process, under the title of waviness. Geometric imperfections are often called waviness if its wavelength is much longer than Hertzian contact width. In this paper, a system of a flexible rotor and two ball bearings with squeeze film dampers and centralizing springs and also consideration of waviness has been modeled and solved by a numerical integration method to investigate the system dynamic response. Results show that by increasing the number of wave lobes, non-periodic and chaotic behavior increases. This reveals the importance of manufacturing accuracy and necessity of taking this term into account in simulations. Moreover, by changing the oil film thickness, it is revealed that there is an optimal value for this parameter to provide maximum damping. In addition, with increasing the inner race mass of SFD, the disc displacement amplitude increases. This reveals the importance of utilizing light materials in manufacturing the SFDs.

Narayana et al. [2] proposed a paper on characteristics investigation of squeeze film damper using triangular element. in it theoretical analysis for finite squeeze film damper using finite element method is presented. The modified Reynolds equation in the film is solved using the finite element discretization. A Galerkin variational method is applied for solving modified Reynolds equation to determine the pressures as well as load carrying capacities. The pressure distribution and load carrying capacity of the squeeze film damper is obtained for different length to diameter ratios and eccentricity ratios for half film condition.

MOHAN et al. [3] presented a paper on design of squeeze film damper supports for rigid rotors. He investigates squeeze film bearings supporting a centrally preloaded rigid rotor mounted in antifriction bearings. Assuming the short bearing approximation and isothermal, incompressible lubrication, design data are presented for such a system over a wide range of operating conditions. The design considerations include the possibility of undesirable operation modes, the maximum imbalance for which the squeeze film support is superior to the rigid mount, the transmissibility at design speed and the forces transmitted during start-up. It is shown that unbalance force attenuations by factors of three or more are a practical possibility with a consequent increase in antifriction bearing life.

Zhu et al.[4] proposed a paper on analysis of the multiple-solution response of a flexible rotor supported on non-linear squeeze film dampers. It is proposed that the behaviour of the multiple-solution response in a flexible rotor supported on two identical squeeze film dampers with centralizing springs is studied by three methods: synchronous circular centred-orbit motion solution, numerical integration method and slow acceleration method using the assumption of a short bearing and cavitated oil film the differences of computational results obtained by the three di!erent methods are compared in this paper. It is shown that there are three basic forms for the multiple-solution response in the flexible rotor system supported on the squeeze film dampers, which are the resonant, isolated bifurcation and swallowtail bifurcation multiple solutions. In the multiple-solution speed regions, the rotor motion may be subsynchronous, supersubsynchronous, almost-periodic and even chaotic, besides synchronous circular centred, even if the gravity effect is not considered.

Khalida et al.[5] presented a paper on an experimental study on steel and teflon squeeze film dampers. In this paper, the vibration analysis on Teflon and steel squeeze film dampers has been carried out. At different frequency ranges, vibration amplitude and the resonance frequency are measured. The eccentricity ratio at resonance speed has been determined. Results show that the vibration amplitude of the steel damper is 10% less at resonance compared with the teflon damper.

Bouzidane et al.[6] presented a paper nonlinear dynamic analysis of a rigid rotor supported by a three-pad hydrostatic squeeze film dampers. In this article he has studied the nonlinear dynamic behaviour of rigid rotors, supported by a new hydrostatic squeeze film damper (HSFD). A nonlinear model of an HSFD is presented. The results are compared with those obtained from a linear approach that is only valid for small vibrations around the equilibrium position. Compared to the four-pad HSFD, the advantage of using a three-pad HSFD consists of reducing the cost due to the need for a feeding system and the volumetric flow rate used in hydrostatic lubrication. In this study, the effects of the pad dimensions ratios, capillary diameters, and rotational speed on the flow rate, unbalance responses, and transmitted forces are investigated using a nonlinear method and the results are analyzed and discussed. The results obtained show that this type of HSFD provides hydrostatic designers with a new bearing configuration suitable to control rotor vibrations and bearing transmitted forces for high speeds.

Borutzky et al.[7] proposed a paper on bond graph modelling and simulation of multidisciplinary systems – an introduction. This paper introduces a graphical, computer aided modelling methodology that is particularly suited for the concurrent design of multidisciplinary systems, viz. of engineering systems with mechanical, electrical, hydraulic or pneumatic components, including interactions of physical effects from various energy domains. Following the introduction, bond graph modelling of multibody systems, as an example of an advanced topic, is briefly addressed in order to demonstrate the potential of this powerful approach to modelling multidisciplinary systems. It is shown how models of multibody systems including flexible bodies can be built in a systematic manner.

19

Kumar et al[8] proposed a paper on development of smart squeeze film dampers for small rotors. In this paper, a typical SFD is designed and development using MR fluid and tested for different amount of damping. It is observed that the damping provided by MR fluid increases with increase in magnetic field and the amplitude of vibration reduces by 70% at critical speeds.

Faris et al.[9] proposed a paper on experimental investigation of the dynamic response of squeeze film dampers made of steel and glass/epoxy. This work is devoted to the fabrication and investigation of the squeeze film dampers (SFDs) which are widely used in many applications. This include the fabrication of a test rig and several dampers with different sizes and two different materials which composite and non-composite. Composite dampers (Glass/epoxy), each consists of 30 layers, were fabricated by hand lay-up method. Outer and inner diameters of all the fabricated dampers were maintained as 60 and 40 mm respectively. Non-composite dampers (Steel) were fabricated and tested using turning machine. Three dampers of different lengths were examined for both materials. A rotor-bearing system for the analysis has been designed and fabricated. The test rig consists of mild steel shaft, two supports, oil pressure system, and two self-alignment ball bearings were fixed on each end support. Two squeeze film dampers were used for the two support ends. Vibration amplitude has been examined for all the fabricated dampers at different shaft rotational speeds. The first resonance speed was examined for all the dampers tested. Results show that the vibration amplitude of the steel damper was lower than Glass/epoxy dampers with the same L/D ratio. On the other hand, a considerable weight saving has been achieved by using Glass/epoxy composite dampers. It has been found that the performance of squeeze film damper improved with increasing length/diameter ratio (L/D) within the range tested.

Cao et al.[10] presented a paper on Numerical analysis of flexible rotor with nonlinear bearings and squeeze film dampers. In this paper dynamic behaviors of a flexible rotor supported on nonlinear bearings and nonlinear squeeze film dampers. The nonlinear bearing and damper forces, which depend on instantaneous nodal displacements and velocities, are calculated at each time step through closed form solutions of Reynolds equation. Such combinations of fluid film bearings and

squeeze film dampers are often used in industrial machines such as compressors and steam turbines to increase system damping. To describe the coupled motion of shaft, bearing and squeeze film damper, a method of assembling both the linear rotor and the nonlinear components is developed. The numerical transient analyses are applied to a 3-disk rotor supported with nonlinear short plain journal bearings and nonlinear short squeeze film dampers. Squeeze film dampers, introduced to the system, increase dynamic stability of the system under a wide range of system rotational speeds, and decrease the bearing forces under severe unbalance forces. Different nonlinear rotor dynamic behavior, such as sub-harmonic, super-harmonic and torus orbits are shown in transient analyses. This type of analysis can be employed to study whether a centering spring is required in the damper or not.

Dousti et al[11]. proposed a paper on a numerical cfd analysis on supply groove effects in high pressure, open end squeeze film dampers. In this paper, we address the supply groove depth and pressurization effects on the behavior of open end squeeze film dampers using numerical CFD approach. A steady state moving reference frame technique, rather than a full time transient one, is implemented in this study, which allows shortening the computation time significantly and to be able to examine more cases readily. Our findings show that significant fluid motion takes place in the supply groove causing its pressure to be varying mainly in circumferential direction and be lower than the supply pressure, in general. The supply holes configuration plays an important role in pressure profile both in groove and land region, especially when the supply groove is shallow. Mid land grooves may have significant dynamic contribution to squeeze film dampers despite their large depth. There exists an optimal supply groove depth which renders the squeeze film damper most effective. In higher rotational speeds and shallow supply grooves, negative pressure values and cavitation phenomenon appear which defeats the purpose of pressurization to a certain extent.

Rodrigues et al.[12] presented a paper on interaction of squeeze film dampers and hole feed systems and its influence on the dynamics of a jeffcott rotor. The model developed in the present work is based on the application of the simplified form of the energy equation commonly used in hydraulics, with approximate pressure drop coefficients. As a boundary condition we impose the power supplied

21

to the pump. The nonlinear hydraulics problem is coupled with the squeeze flow and the Newton–Raphson method is employed to solve the set of nonlinear equations. The influence of the hole feed system on the unbalance response and stability of a Jeffcott rotor is analyzed in regards to the number of feed holes and the power supplied to the pump. The feed system behavior is also studied.

Bouzidane et al. [13] presented a paper on nonlinear dynamic behavior of a rigid rotor supported by hydrostatic squeeze film dampers. This research project aims to study the nonlinear dynamic behavior of a rigid rotor supported by hydrostatic squeeze film dampers (HSFDs). The investigated HSFD consists of four hydrostatic bearing flat pads fed by capillary restrictors. A nonlinear hydrostatic squeeze film damper model is developed, and the results are compared with those obtained using a linear approach. The effect of unbalance eccentricity on the vibration response and the transmitted force of the HSFD are investigated using the linear and nonlinear models. The results show good agreement between the linear and nonlinear methods when the unbalance force is small. However, as the unbalance forces become larger, the results obtained using the linear models cease to be representative of the real behavior of rotor dynamics and a nonlinear approach must be conducted. The effects of supply pressure, viscosity, pressure ratio, and rotational speed on the response and the force transmitted to the HSFD are investigated using a nonlinear approach.

Moraru et al.[14] presented a paper on the design of squeeze film dampers operating within the limits of the Reynolds theory.In This paper discuss some design aspects as well as modeling aspects of the SFD that operate within the limits of the classical Reynolds theory. The behavior of a SFD depends on the flow within the oil film. The supply and drain systems together with the sealing system impose the ratio between the axial flow rate and the radial flow rate as well as the pressure in the negative squeeze area. Vapor cavitation may occur (which can be destructive), however, gaseous phenomena can be controlled by providing larger amounts of oil at higher pressures. Flexibility provided by damping can reduce the dynamic load transmitted through the bearings provided that supports are made soft enough to keep the undamped critical speed considerably less than 70%, however, wrong selected dampers can have a detrimental effect.

Lin et al. [15] presented a paper on squeeze film characteristics of long partial journal bearing lubricated with couple stress fluid. In this paper he has devised on the basis of microcontinuum theory, a theoretical anaiysis of hydrodynamic squeeze film behaviour for long partial journal bearings lubricated by fluids with couple stresses is presented. To take into account the couple stress effects due to the lubricant containing additives or suspended particles, the modified Reynolds equation governing the film pressure is derived by using the Stokes consitutive equations. Various bearing characteristics are then calculated. According to the results obtained, the influence of couple stress effects on the performance of the system is physically apparent and not negligible. compared with the Newtonian lubricant case, the couple stress effects provide an enhancement in the load-carrying capacity and lengthen the response time of the squeeze film action. On the whole, the presence of couple stresses signifies an improvement in the squeeze film characteristics of the system.

Guo et al. [16] proposed a paper on application of CFD analysis for rotating machinery, part 1: Hydrodynamic, hydrostatic bearings and squeeze film damper. In this paper some of the capabilities in CFX-TASCflow are applied to simulate the pressure field and calculate the static and dynamic characteristics of hydrodynamic, hydrostatic and hybrid bearings as well as squeeze film dampers. The comparison between the CFD analysis and current computer programs used in industry has been made. The results show reasonable agreement in general.

SALBU et al. [17] proposed a paper on compressible squeeze films and squeeze bearings. In this paper experimental agreement with a finite-difference solution of the isothermal squeeze film equation was obtained for steady-state sinusoidal squeeze motion of parallel, coaxial disks. At low squeeze number, the film force is in phase with the velocity; at high squeeze number, with the displacement. Compressibility effects at high squeeze number introduce a superambient mean pressure, so that it is possible to operate a gas bearing on squeeze effects alone. Thrust bearings, spherical bearings, and- journal bearings have been successfully operated as squeeze bearings, using both electromagnetic and piezoelectric devices to generate the squeeze motion.

Proctor et al. [18] presented a paper on nonlinear whirl response of a high-speed seal test rotor with marginal and extended squeeze-film dampers. In this research paper synchronous and nonsynchronous whirl response analysis of a double overhung, high-speed seal test rotor with ball bearings supported in 5.84 and 12.7 mm-long, un-centered squeeze-film oil dampers is presented. Test performance with the original damper of length 5.84 mm was marginal, with non synchronous whirling at the overhung seal test disk and high amplitude synchronous response above 32,000 rpm near the drive spline section occurring. A system critical speed analysis of the drive system and the high-speed seal test rotor indicated that the first two critical speeds are associated with the seal test rotor. Nonlinear synchronous unbalance and time transient whirl studies were conducted on the seal test rotor with the original and extended damper lengths. With the original damper design, the nonlinear synchronous response showed that unbalance could cause damper lockup at 33,000 rpm. Alford cross coupling forces were also included at the overhung seal test disk for the whirl analysis. Sub-synchronous whirling at the seal test disk was observed in the nonlinear time transient analysis. With the extended damper length of 12.7 mm, the sub-synchronous motion was eliminated and the rotor unbalance response was acceptable to 45,000 rpm with moderate rotor unbalance. However, with high rotor unbalance, damper lockup could still occur at 33,000 rpm, even with the extended squeeze-film dampers. Therefore, the test rotor must be reasonably balanced in order for the un-centered dampers to be effective.

Gunter et al. [19] presented a paper on whirl motion of a seal test rig with squeeze-film dampers. This paper presents the experimental behavior and dynamic analysis of a high speed test rig with rolling element bearings mounted in squeeze film oil damper bearings. The test rotor is a double overhung configuration with rolling element ball bearings mounted in uncentered squeeze-film oil dampers. The damper design is similar to that employed with various high-speed aircraft HP gas turbines. The dynamic performance of the test rig with the originally installed dampers with an effective damper length of length 0.23-inch was unacceptable. The design speed of 40,000 RPM could not be safely achieved as non synchronous whirling at the overhung seal test disk and high amplitude critical speed response

at the drive spline section occurred at 32,000 RPM. In addition to the self excited stability and critical speed problems, it was later seen from FFT data analysis, that a region of super synchronous dead band whirling occurs between 10,000 to 15,000 RPM which can lead to bearing distress and wear. The system was analyzed using both linear and nonlinear techniques. The extended length damper design resulting from the analysis eliminated the rotor subsynchronous whirling, high amplitude critical speed, and the dead band whirling region allowing the system to achieve a speed of 45,000 RPM. However, nonlinear analysis shows that damper lockup could occur with high rotor unbalance at 33,000 RPM, even with the extended squeeze-film dampers.

Shende et al. [20] .has presented a paper on squeeze film damping for aircraft gas turbines. In it modern aircraft gas turbine engines depend heavily on squeeze film damper supports at the bearings for abatement of vibrations caused by a number of probable excitation sources. This design ultimately results in light-weight construction together with higher efficiency and reliability of engines. Many investigations have been reported during past two decades concerning the functioning of the squeeze film damper, which is simple in construction yet complex in behaviour with its non-linearity and multiplicity of variables. These are reviewed in this article to throw light on the considerations involved in the design of rotor-bearing-casing systems incorporating squeeze film dampers.

Heidari et al. [21] presented a paper on the influence of asymmetry in centralizing spring of squeeze film damper on stability and bifurcation of rigid rotor response. In this paper, stability and bifurcation of the unbalance response of a rigid rotor supported by squeeze film damper with asymmetry in centralizing spring are investigated. The unbalanced rotor response is determined by the shooting method and the stability of these solutions is examined by using the Floquet theorem. Numerical examples are given for both symmetric ($k_x = k_y$) and asymmetry ($k_x \neq k_y$) centralizing springs in x or y direction. Jump phenomenon and sub-harmonic and quasi-periodic vibrations are predicted for a range of design and operating parameters such as the unbalancing (U), gravity (W), bearing (B) and spring (K). The results show that increasing the spring stiffness

asymmetry parameter in y direction has no influence on the nature of system response and occurrence of bifurcation. But, examining the effect of increase in stiffness parameter in x direction leads to occurrence instability and period-doubling bifurcation in response to the system. Our findings show that this phenomena are due to the weight force in the y direction. Finally, it is shown that the unsymmetrical stiffness of squeeze film dampers in the presence of cavitation promoting the chance of undesirable non synchronous vibrations.

2.3 Research gap in literature

 Reasearcher have done various study regarding the effect of squeeze film damper on the vibration amplitude of rotor shaft .They have done it through experiments and with software tools . But there is not much study on effect of squeeze film damper on vibration amplitude of shaft with rotor with the help of bond graph technique and also the effect of variation in various parameters of squeeze film damper on vibration amplitude is not studied earlier. So ,in this thesis the study of effect of squeeze film damper with the help of bond graph technique is being carried out and the detailed analysis of various parameters of squeeze film damper is done.

CHAPTER -3

MATHEMATICAL MODELLING

3.1 Introduction

A mathematical model of a dynamic system is defined as a set of equations that represent dynamics of system accurately or at least fairly well. A mathematical system not unique to a given mechanical system . A system may be represented in different ways and therefore may have many mathematical models , depending on one's perspective .

The dynamics of a mathematical model can be described in terms of differential equations. Such differential equations may be obtained by using physical laws governing particular system for example Newton's used in case of mechanical system and Renoldys equation in hydraulic system. Mathematical model may as you may give many different forms. Depending on the particular system and the particular circumstances, one mathematical model may be better suited than other models. Once a mathematical model of a system is obtained various analytical and Computer tools can be used for analysis and synthesis purposes .

This chapter presents the mathematical modelling of the rigid rotor on squeeze film damper with centralizing spring.

3.2 Mathematical modelling of squeeze film damper

Oil film forces are a key factor in the modeling of the fluid film of squeeze film dampers. Components of the oil film forces in squeeze film damper can be obtained by integrating the pressure distribution over the inner surface of the damper. The damper pressure distribution is derived through Reynolds equation by following simple assumptions:

1. The oil film thickness is small compared to the radius of the journal. So, the curvature of the oil film is negligible.

2. The pressure gradient along the oil film thickness (in a radial direction) is small, and it is ignored.

3. The velocity gradient along the oil film thickness (in a radial direction) is small, and it is ignored. In fact, the lubricant fluid flow is a two-dimensional.
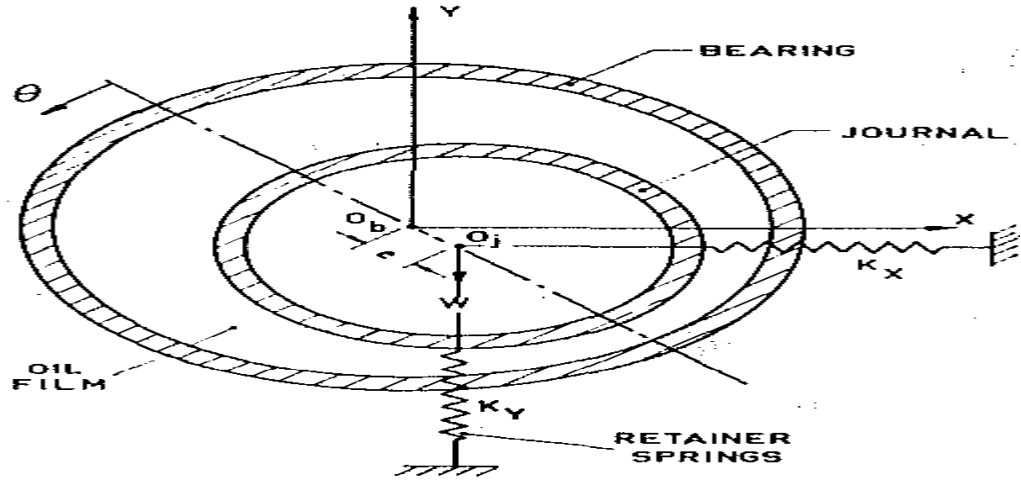

Figure 3.1:- Squeeze film bearing support representation [3]

4. Since the lubricant fluid flow is steady, the internal forces acting on the fluid elements are ignored.

5. The volume forces acting on the particles of fluid are neglected.

6. It is assumed that the lubricant fluid flow is laminar.

7. The extent of the positive pressure region is the same for completed and ruptured films.

As mentioned, the pressure distribution of a short damper with cavitation (p-film model) is derived from the Reynolds equation. This distribution in a rotating coordinate system is as follows.

$$P(\theta, z) = \frac{6\mu}{c^2}\left(z^2 - \frac{L^2}{4}\right)\left(\frac{\varepsilon\dot{\varphi}\sin\theta + \dot{\varepsilon}\cos\theta}{(1+\varepsilon\cos\theta)^3}\right) \tag{3.1}$$

where L is damper length, c is radial clearance of damper, z is axis coordinate of the damper, μ is the dynamic viscosity of lubricant, and ε and $\dot{\varepsilon}$, represent the displacement and velocity in radial direction, respectively. In addition, $\dot{\varphi}$ represents the angular velocity, and h is angular coordinate measured from the location of maximum thickness of the oil film in the direction of the angular velocity of the rotor damper.
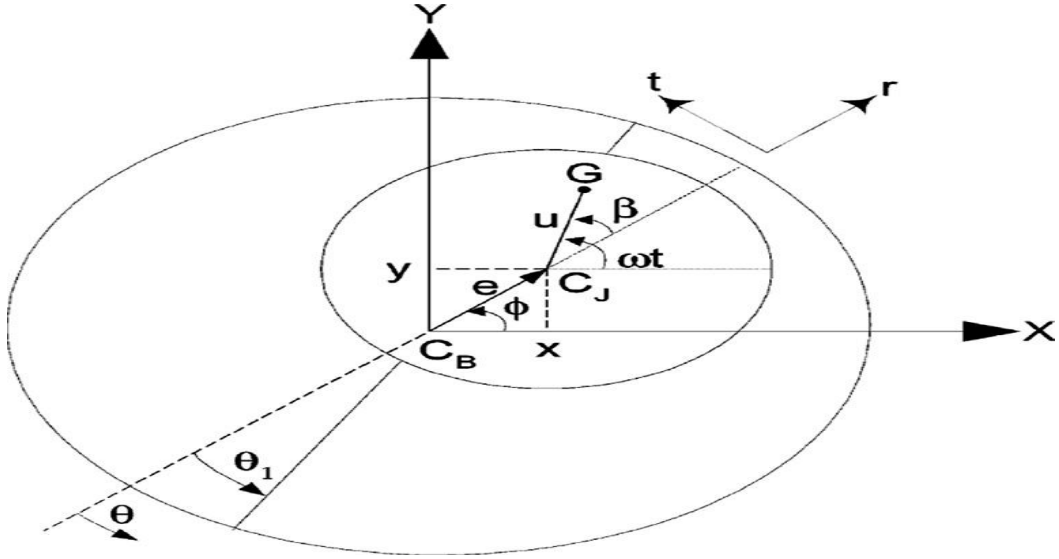
Figure 3.2 : Coordinate systems used to find the equation of motion [21]

Positive pressures occur for $\theta_1 < \theta < \theta_1 + \pi$

$$\varepsilon\dot{\varphi}\,sin\theta + \dot{\varepsilon}cos\theta > 0$$

$$tan\theta_1 = \frac{-\dot{\varepsilon}}{\varepsilon\varphi} \qquad (3.2)$$

Components of the oil film forces in polar coordinates can be integrated from the pressure distribution at all inner faces of the damper and calculated as a function of ε, $\dot{\varepsilon}$ and $\dot{\varphi}$expressed in following equations.

$$F_r = R \int_{\theta_1}^{\theta_1+\pi} \int_{\frac{-L}{2}}^{\frac{L}{2}} P cos\theta \; d\theta \; dz = \frac{-\mu R L^3}{c^2}(\varepsilon\dot{\varphi}\; I_1 + \dot{\varepsilon}I_2) \qquad (3.3)$$

$$F_t = R \int_{\theta_1}^{\theta_1+\pi} \int_{\frac{-L}{2}}^{\frac{L}{2}} P sin\theta \; d\theta \; dz = \frac{-\mu R\, L^3}{c^2}(\varepsilon\dot{\varphi}\; I_3 + \dot{\varepsilon}I_1) \qquad (3.4)$$

Where

29

$$I_1 = \int_{\theta_1}^{\theta_1 + \pi} \frac{sin\theta \, cos\theta}{(1+cos\theta)^3} \, d\theta \qquad (3.5)$$

$$I_2 = \int_{\theta_1}^{\theta_1 + \pi} \frac{cos^2\theta}{(1+cos\theta)^3} \, d\theta \qquad (3.6)$$

$$I_3 = \int_{\theta_1}^{\theta_1 + \pi} \frac{sin^2\theta}{(1+cos\theta)^3} \, d\theta \qquad (3.7)$$

To extract the differential equations that govern the system, we need the components of the oil film in the Cartesian coordinates. These components can be easily transferred to Cartesian coordinates by using the following equations.

$$F_{DX} = F_r cos\varphi - F_t sin\varphi \qquad (3.8)$$
$$F_{DY} = F_r sin\varphi + F_t cos\varphi \qquad (3.9)$$

3.3 Rayleigh beam model

As the bondgraph model of rotor shaft is based on Rayleigh beam model. That's why, the mathematical modelling of Rayleigh beam is described here.

The following assumptions are taken into consideration:

i. The Beam is prismatic and has a straight centroidal axis (which we will label the x-axis),

ii. The beam's cross-section has an axis of symmetry (which we will label the y axis)

iii. All transverse loading act in the plane of symmetry(x-y plane),

iv. Plane sections perpendicular to the centroidal axis remains plane after deformation,

v. The material is elastic, isotropic an homogeneous,

vi. Transverse deflections are small.

.

The physical situation is drawn schematically in Figure 3.3. On may denote the internal bending moment moment by M, the internal shear force by V and the external loading distributed loading by w.
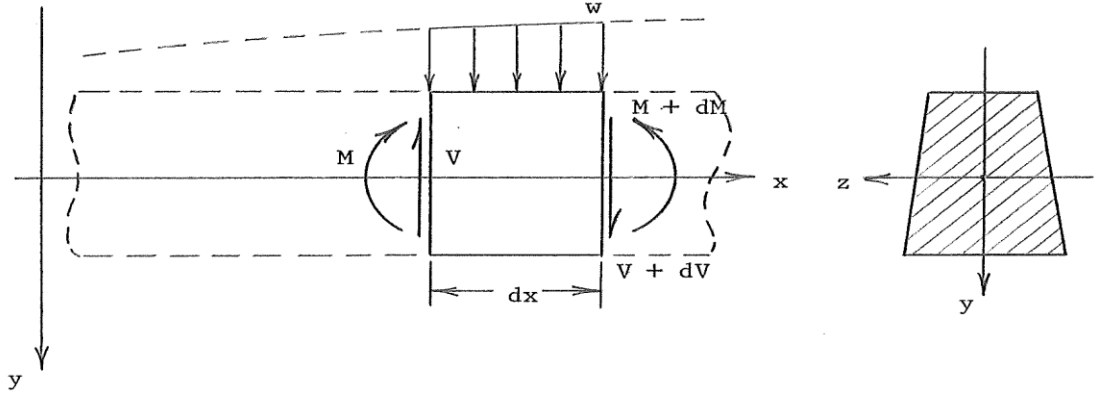
Figure 3.3 : Beam element with generalized forces and displacement

The elementary Euler- Bernoulli beam theory has some serious shortcomings for high frequency motion. One can make here a refinement in the story to account for the rotary motion of beam elements. This rotary connection was first applied by Rayleigh and hence the same terminology Rayleigh beam theory is used here.

The place where the rotary motion, i.e., the angular acceleration of beam elements, would be incorporated into the analysis lies in the moment equation (3.10)

$$\frac{\partial M}{\partial x} = V \tag{3.10}$$

Taking this motion into account,(2.10) now would read

$$\frac{dM}{dx} = V - \rho I \frac{\partial^2 \theta}{\partial t^2} \tag{3.11}$$

where θ is the angle of rotation of the beam element, and ρ and I as before being the material density and cross sectional area moment of inertia respectively. For small deformation $\cong \frac{dy}{dx}$, and so (3.11) becomes

$$\frac{dM}{dx} = V - \rho I \frac{\partial^3 y}{\partial t^2 \, \partial x} \tag{3.12}$$

$$\frac{dV}{dx} = -w + \rho A \frac{\partial^2 y}{\partial t^2} \tag{3.13}$$

31

Combining equation (3.13) and (3.12) with (3.10) gives

$$b^2 \frac{\partial^4 y}{\partial x^4} - a^2 \frac{\partial^4 y}{\partial x^2 \partial t^2} + \frac{\partial^2 y}{\partial t^2} = 0 \tag{3.14}$$

where we have taken the zero external loading case, $b^2 = \frac{EI}{\rho A}$ and $a^2 = \frac{I}{A}$. Equation (3.14) is then the governing relations for Rayleigh beam theory.

The separation of variables method may also be applied successfully to equation (3.14). Putting in the product form $y = X(x)T(t)$, gives

$$x'''' + \frac{\gamma^2 a^2}{b^2} x'' - \frac{\gamma^2 x}{b^2} = 0 \tag{3.15a}$$

$$\ddot{T} + \gamma^2 T = 0 \tag{3.15b}$$

Here is γ again the separation constant.

The solution to (3.15) is the same as for the Euler-Bernouli case, the solution is not quite so easy, but can be handled by putting in a solution form Ae^{rx} .After cancelling common terms this produces the characteristic equation.

$$r^4 + \frac{\gamma^2 a^2}{b^2} r^2 - \frac{\gamma^2}{b^2} = 0 \tag{3.16}$$

The roots of this equation are

$$r_{1,2} = \pm\{-\frac{\gamma^2 a^2}{2b^2} - \left[\frac{\gamma^4 a^4}{4b^4} + \frac{\gamma^2}{b^2}\right]^{\frac{1}{2}}\}^{1/2} \tag{3.17a}$$

$$r_{3,4} = \pm\{-\frac{\gamma^2 a^2}{2b^2} + \left[\frac{\gamma^4 a^4}{4b^4} + \frac{\gamma^2}{b^2}\right]^{\frac{1}{2}}\}^{1/2} \tag{3.17b}$$

So our solution may be written as

$$X(x) = A_1 e^{r_1 x} + A_2 e^{r_2 x} + A_3 e^{r_3 x} + A_4 e^{r_4 x} \tag{3.18}$$

Or by letting $r_{1,2} = \pm im_1$ and $r_{3,4} = \pm im_2$, we write

$$\begin{aligned} X(x) &= C_1 \sin m_1 x + C_2 cos m_1 x \\ &= C_3 \sin m_2 + C_4 cos m_2 x \end{aligned} \qquad (3.19)$$

Notice that the Rayleigh solution from, (3.19) is quite similar to the Euler-Bernouli results. However a detailed comparison of the frequencies and mode shapes would show a difference between the two theories.

3.4 Mathematical model of bearing support

In some rotating machines, e.g. turbines, bearings themselves may be mounted on flexible foundations (Figure 3.4), which may in turn influence the motion of disc masses. In the present section, a very simple model of the foundation is considered by ignoring cross-coupled terms of the stiffness and the damping.

The net displacement of the disc is given by the vector sum of (i) the disc displacement relative to shaft ends, plus (ii) that of shaft ends relative to the bearing, plus (iii) that of the bearing relative to the space. The theoretical analysis of the disc, the shaft and the bearing responses, and that of the force transmissibility of such a system, can be carried out in a similar manner to that described in the previous section. Additional governing equations related to the foundation are derived, and how to relate them with governing equations of the disc and bearings are detailed here.
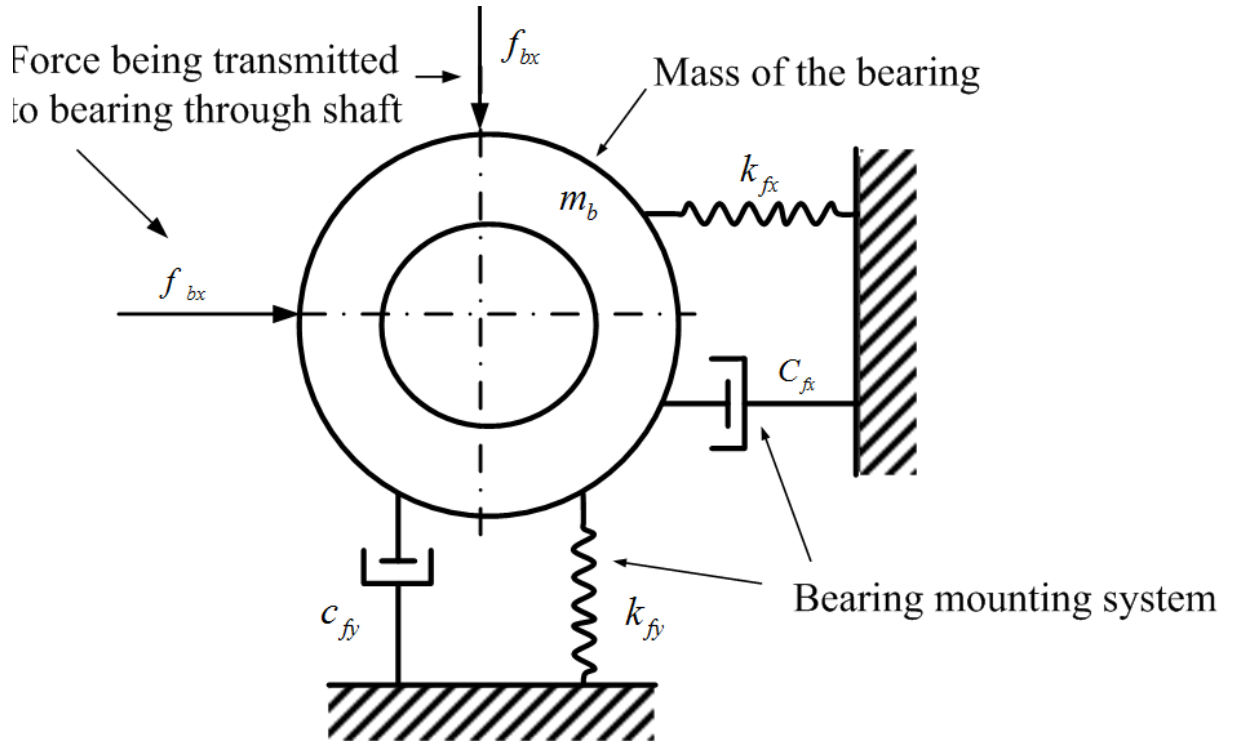
Figure 3.4: A bearing block mounted on a foundation

The bearing will respond in the horizontal direction for an external force f_{bx}, which is governed by the following equation

$$f_{by} - K_{fx} \cdot x_f - C_{fx} \cdot \dot{x}_f = m_b \cdot \ddot{x}_f \tag{3.20}$$

where x_f is the horizontal displacement of the bearing, m_b is the bearing mass of one bearing and $K_{fx}, C_{fy}, K_{fy}, C_{fx}$ are the foundation stiffness and damping coefficients.

Similarly, the response of the bearing in the vertical direction to a force *fby* is given as

$$f_{by} - K_{fy} \cdot y_f - C_{fy} \cdot \dot{y}_f = m_b \ddot{y}_f \tag{3.21}$$

where y_f is the vertical displacement of bearing. The displacement of the bearing will take the form.

$$x_f = X_f \cdot e^{j\omega t} \qquad \text{and} \quad y_f = Y_f \cdot e^{j\omega t} \tag{3.22}$$

On substituting equation (3.22) in equations of motion (3.21) and (3.20), and on combining in the matrix form , it gives

$$[D][X_f] = [F_b] \tag{3.23}$$

Where,

$$[D] = \left(\begin{bmatrix} K_{fx} & 0 \\ 0 & K_{fy} \end{bmatrix} - \omega^2 \begin{bmatrix} m_b & 0 \\ 0 & m_b \end{bmatrix} + jw \begin{bmatrix} C_{fx} & 0 \\ 0 & C_{fy} \end{bmatrix} \right) \tag{3.24}$$

$$\{X_f\} = \begin{Bmatrix} x_f \\ y_f \end{Bmatrix} \tag{3.25}$$

and $\quad \{F_b\} = \begin{Bmatrix} F_{bx} \\ F_{by} \end{Bmatrix} \tag{3.26}$

which gives relative displacements between bearings and the foundation, as

$$\{X_f\} = [D]^{-1}\{F_b\} \tag{3.27}$$

Forces transmitted to foundations are given as

$$f_{fx} = k_{fx}.x_f + c_{fx}.\dot{x}_f \tag{3.28}$$

$$f_{fy} = k_{fy}.x_f + c_{fy}.\dot{x}_f \tag{3.29}$$

For the unbalance excitation, we have

$$f_{fx}=F_{fx.}e^{j\omega t} \qquad \text{and} \qquad f_{fx} = F_{fy.}e^{j\omega t} \tag{3.30}$$

On substituting equation (3.30) into equation (3.29) and (3.28), we get

$$\begin{Bmatrix} F_{fx} \\ F_{fy} \end{Bmatrix} = \left(\begin{bmatrix} k_{fx} & 0 \\ 0 & k_{by} \end{bmatrix} + j\omega \begin{bmatrix} c_{fx} & 0 \\ 0 & c_{fy} \end{bmatrix} \right) \begin{bmatrix} X_f \\ Y_f \end{bmatrix}$$

Forces transmitted through foundations will not be the same as forces transmitted through bearings. Since bearing masses (i.e., inertia forces) will absorb some forces towards its acceleration. If bearing masses are negligible then bearings and foundations will transmit same amount of forces, however, may be with some

35

phase lag due to damping. The amplitude and the phase of forces transmitted through foundations can be calculated.

3.5 Mathematical modeling of the rigid rotor system with squeeze film damper

The Rotor (with mass 2 m) is placed on one ball bearings and two one squeeze film damper. Each damper has a centralizing spring This work presents spring stiffness of the squeeze film damper with values in two directions (x, y) and obtains K_x , K_y. The Pure static unbalance is demonstrated by the eccentricity of the rotor (u). This factor is related to the distance of mass center of the rotor (G) and is measured by the geometric center of rotation. In the case of rigid rotor, the geometric centers of rotation and journal $((C_j)$ are the same. To obtain the governing equation of the rigid rotor system with both squeeze film damper and centralizing spring, the following assumptions are considered:

1. The gyroscopic effect is neglected.

2. Displacement of the rotor in the axial direction is neglected.

3. The centralizing spring is considered as linear spring.

4. Excitation forces of the ball bearings are neglected.

The governing equation of the system is obtained in coordinate (x, y) due to the displacement of the geometric center of the journal in the bearing housing. According to external forces of the oil film, gravity and unbalance force, governing equations of the journal motion are as follows:

$$m\ddot{x} = F_{DX} - K_x x + mu\omega^2 \cos\omega t \tag{3.31}$$

$$m\ddot{y} = F_{DY} - K_y y - mg + mu\omega^2 \sin\omega t \tag{3.32}$$

Dimensionless differential equations that governs the rigid rotor system with squeeze film damper and asymmetric centralizing spring will be as follows:

$$\ddot{X} = -B\left[\frac{X}{\varepsilon}[I_1\dot{\varepsilon} + I_2\varepsilon\dot{\varphi}] - \frac{Y}{\varepsilon}[I_2\dot{\varepsilon} + I_3\varepsilon\dot{\varphi}]\right] - K_x^2 X + U\cos\tau \tag{3.33}$$

$$\ddot{Y} = -B\left[\frac{Y}{\varepsilon}[I_1\dot{\varepsilon} + I_2\varepsilon\dot{\varphi}] + \frac{X}{\varepsilon}[I_2\dot{\varepsilon} + I_3\varepsilon\dot{\varphi}]\right] - K_y^2Y - W + U\sin\tau \qquad (3.34)$$

$$B = \frac{\mu RL^3}{m} \quad, K_x = \frac{\omega_{nx}}{\omega} \quad, \qquad K_y = \frac{\omega_{ny}}{\omega} \quad, U = \frac{u}{c} \quad, \qquad W = \frac{g}{w^2c}$$

B, U, W, K_x and K_y are dimensionless parameters of the system.

3.6 Summary of the chapter

In this chapter mathematical modelling of different components used in our analysis is done. The mathematical modelling of squeeze film damper is done with the help of Reynolds equation. The mathematical modelling of rotor shaft is done based on Rayleigh beam model. A simplified mathematical model of bearing support is modelled by ignoring cross coupled terms of stiffness and damping and last section mathematical modelling of rigid rotor system with squeeze film damper is done. The nomenclature presents all the notation used in the mathematical model. The mathematical model obtained in this chapters are used in bond graph modelling of components in the next chapter.

CHAPTER 4

BOND GRAPH MODELLING

4.1 Introduction

A bond graph is a graphical representation of a physical dynamic system. It is similar to the better known block diagram and signal-flow graph, with the major difference that the arcs in bond graphs represent bi-directional exchange of physical energy, while those in block diagrams and signal-flow graphs represent uni-directional flow of information. Also, bond graphs are multi-energy domain (e.g. mechanical, electrical, hydraulic, etc) and domain neutral. This means a bond graph can incorporate multiple domains seamlessly.

The bond graph is composed of the "bonds" which link together "single port", "double port" and "multi port" elements (see below for details). Each bond represents the instantaneous flow of energy (dE/dt) or power. The flow in each bond is denoted by a pair of variables called 'power variables' whose product is the instantaneous power of the bond. For example, the bond of an electrical system would represent the flow of electrical energy and the power variables would be voltage and current, whose product is power. Each domain's power variables are broken into two types: "effort" and "flow". Effort multiplied by flow produces power, thus the term power variables. Every domain has a pair of power variables with a corresponding effort and flow variable. Examples of effort include force, torque, voltage, or pressure; while flow examples include velocity, current, and volumetric flow. The table below contains the most common energy domains and the corresponding "effort" and "flow".

A bond graph has two other features which is derived describe briefly here , and further discussed in more details. One is the "half Arrow" sign convection, which defines the assumed directions of positive energy flow. As with free body diagrams and electrical circuit diagrams, the choice of positive direction is arbitrary with a caveat that analyst must be consistent throughout with chosen definitions. The other feature is the "causal stroke" which is a vertical bar placed on only one end of the Bond and it is not arbitrary. There are rules for signing the

proper causality to a given port and rules for the precedence among ports. In Bond graph any port (single, double or multiple) attached to the bond will specify either "flow" or "effort" by its causal stroke but not both. The port attached at the end of the Bond with a "causal stroke" specifies the "flow" of the bond and the Bond imposes "effort" upon that port. Similarly the port at the end of without the "causal stroke" imposes "effort" to the bond , whereas the bond imposes "flow" to that port.

The Power term is denoted by the product of effort and flow, i.e

Power=Effort(e) x Flow(f)

Table 4.1: Power variables for different energy domains

Systems	**Effect(e)**	**Flow(e)**
Mechanical	Force(F)	Velocity (v)
	Torque (τ)	Angular velocity (ω)
Electrical	Voltage (V)	Current (i)
Hydraulic	Pressure (P)	Volume flow rate ($\frac{dQ}{dt}$)
Thermal	Temperature (T)	Entropy change rate ($\frac{ds}{dt}$)
	Pressure (P)	Volume change rate($\frac{dV}{dt}$)
Chemical	Chemical potential (μ)	Mole flow rate ($\frac{dN}{dt}$)
	Enthalpy (h)	Mass flow rate ($\frac{dm}{dt}$)
Magenetic	Magneto-motive force (e_m)	Magnetic flux(φ)

Let us now see the difference between a classical approach of physical modeling and a bondgraph approach for modeling a system.
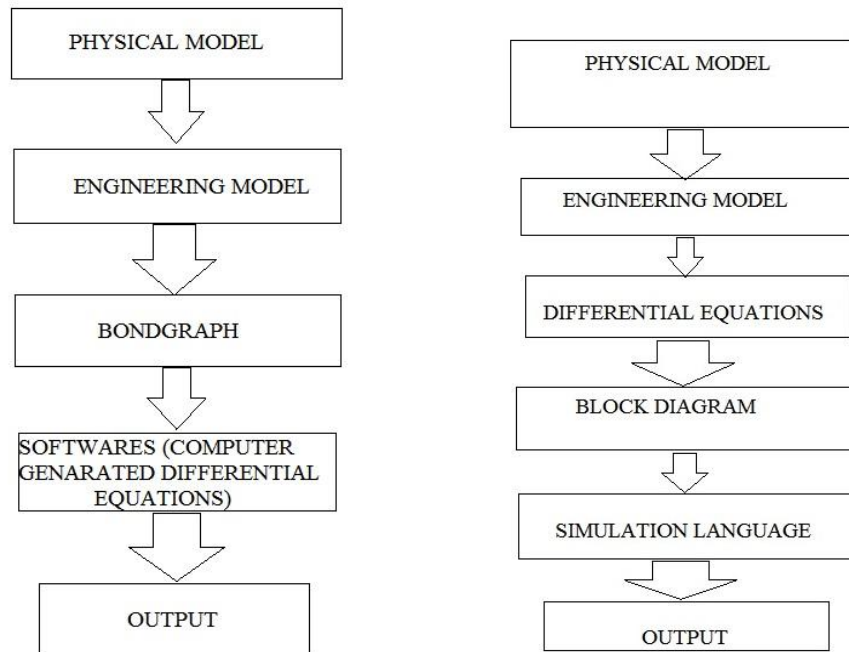

Figure 4.1 (a) Bondgraph Approach   (b) Classical Approach

4.1.1 Basics of Bond graph modelling

The fundamental idea of the bond graph is that power is transmitted between connected components by combination of "flow" and "efforts" (generalized floor and generalized effort). Refer to the Table 4.1 for examples flow and efforts in different domains can be ascertained. If an engine is connected to wheel through a shaft ,the power in the rotational mechanical domain, which means that the flow and efforts are angular velocity (ω) and torque (τ) respectively. The word Bond graph is first step towards the bond graph, in which words define the components . As the word bond graph, this will look like:

$$\text{engine} \xrightarrow{\quad \tau \quad}_{\omega} \text{wheel}$$

To provide a sign convention half arrow is used. If the engine is doing work when τ and ω are positive, then the diagram would be drawn as :

$$\text{engine} \xrightarrow{\quad \tau \quad}_{\omega} \text{wheel}$$

To indicate a measurement of full arrow is used and is referred as single bonds, because the amount of power flowing through the bond is insignificant. However, it may be useful to certain physical components. For example, the power required to activate a relay in orders of magnitude smaller than the power through the itself; making it relevant only to convey whether the which is on, not the power consumed by it .

Wheel ⎯⎯⎯⎯⎯⎯⎯⎯⎯⎯⟶ **tachometer**

(ω)
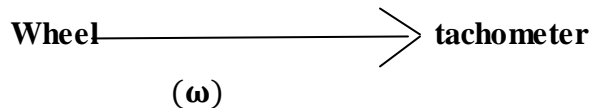
4.1.2 Junction structure in bond graph modelling

Power bonds can join at one of two kinds of junctions i.e. a 1 junction and a 0 junction.

- In a 1 junction, the flows are equal and effort sum to zero. This corresponds to a force balance at a mass in a mechanical system or to electrical loop.

- In a 0 junction the effort are equal and sums to zero. This corresponds to a mechanical "stack" in which all forces are equal or to a node in an electrical circuit (where the Kirchhoff's law is applies).
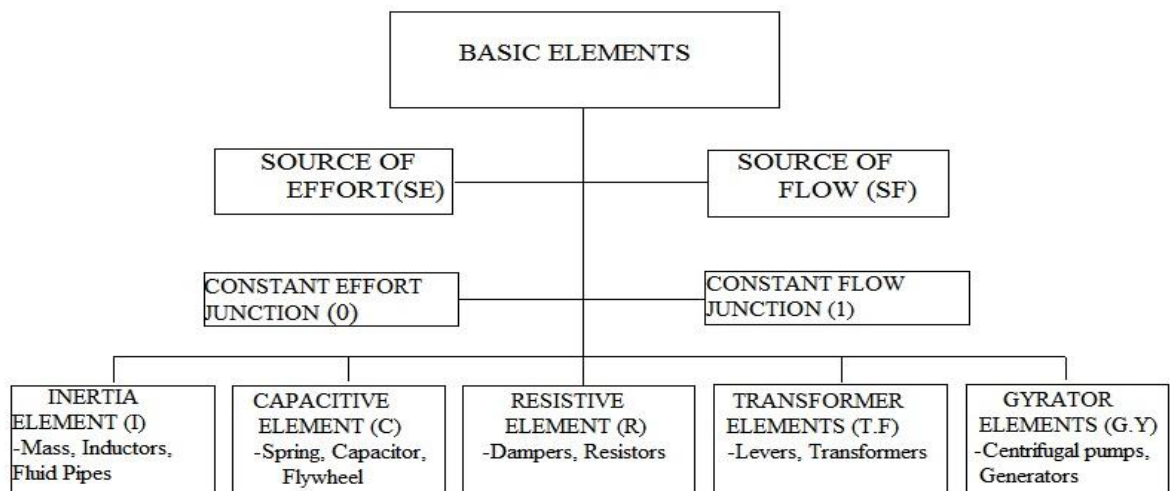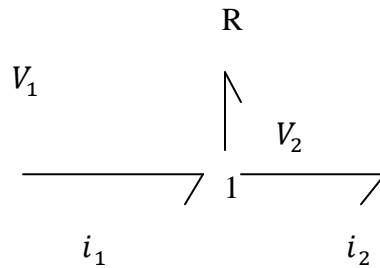

Figure 4.2 :Basic Elements of bond graph modelling

In this case, the flow (current) is constrained to be same at all points, and the efforts sum to zero when the implied current return path is included. Power can be

41

computed at points 1 and 2 whereas in general some power will be dissipated in resistor. Bond graph of this system becomes

$$R$$

$$V_1$$

$$V_2$$

$$i_1 \qquad\qquad 1 \qquad\qquad i_2$$

This diagram maybe seem counter intuitive in that flow which is not preserved in the same way across the diagram, from electrical point of view. It will be helpful to consider the 1 junction as a Daisy chaining the bonds it connects to and the power bond up to R as resistor with a lead turning down. Bond graph modelling proceeds from the identification of key 0 and 1 junctions associated with identifiable flows and efforts in the system, after that indentifying the storage element (I and C) and dissipative (R) , power sources , and drawing bonds wherever the information or Power flows between the junctions, sources and dissipative/ storage components. Then the sign conventions (arrow heads), and after that causality are assigned and finally the questions which is describing the behaviour of a system can be derived using the graph as a kind of map or guide.

4.1.3 Concept of causality in Bond graph modelling

Bond graph have a notion of causality that indicate which side of Bond determines the instantaneous flow and with which side determines the instantaneous efforts. While formulating the dynamic equation which describe the system, causality for each modelling element, which variable is independent and which is dependent. Analysis of a large scale model becomes easier by propagating the causation graphically from one modelling element to other. In a bond graph model, completing causal assignment will allow the detection of a modelling situation where an algebraic loop exists i.e. the situation when a variable is defined recursively as the function of itself.

Considered a capacitor in series with a battery, as an example of causality. To charge a capacitor instantly is not physically possible therefore anything connected in parallel with a capacitor should necessarily have the same voltage (effort variable) as that of the capacitor. Similarly, an inductor cannot

change flux instantly therefore any component connected in series with an inductor should necessarily have the same flow as that at of the inductor. Because inductors and capacitors are passive devices, therefore they cannot maintain their respective flow and voltage indefinitely the components to which they are connected will affect their respective flow and voltage, but only indirectly by affecting their voltage and current respectively. Causality is basically a symmetric relationship. When one side causes flow , the other side causes effort. Active components such as an ideal current or voltage source are also causal.

In a bond graph notation, a causal stroke can be added to one end of the power Bond which indicates that the bond opposite end is defining the effort. For example, consider a constant torque Motors which is driving a wheel , that is a source of effort (SE).

Similarly, the side causal stroke (in case of wheel) defines the flow for the bond. Causality result in the compatibility constraints. It is clear that only one end of the power bond can define the effort therefore only one end of a bond can have a causal stroke. The two passive components with time dependent behaviour , C and I, can only have one sort of causation i.e a C component define effort and I component define flow. Therefore from a Junction J , the only legal configuration for C and I are

$$J \longrightarrow\!\!| \;\; I \quad\quad \text{and} \quad\quad J \;|\!\longrightarrow\!\!\searrow \; C$$

A resistor has no time-dependent behaviour therefore or voltage can be applied to get flow instantly or a be applied to get a voltage instantly.Hence a resister can be at either end of a causal.

$$J \longrightarrow\!\!| \;\; R \quad\quad \text{and} \quad\quad J \;|\!\longrightarrow\!\!\searrow \; R$$

Source of effort (SE) define effort , sources of flow(SF) define flow. Transformers are passive, neither storing energy nor dissipating so the causality passes through them.

A gyrator transform effort to flow and flow to effort, so if effort is caused on one side, flow is caused on the other side and vice versa.
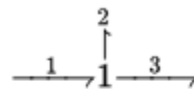

4.1.4 Junction and Causality

In a 1 – junction, flows are equal and in a 0 -junction efforts are equal . Thus, with causal bonds only one bond can cause the flow in a 1- junction and only one can cause the effort in 0 – junction. Therefore if the causality of others is also known .That bond is known as strong bond.
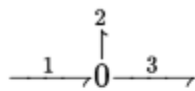
Resulting equations:

$$e_1 = e_2 = e_3$$
$$f_1 = f_2 + f_3$$

Resulting equations:

$$f_1 = f_2 = f_3$$
$$e_1 = e_2 + e_3$$

Using the above our rules one can continue to assign the causality. If any model which results in inconsistent causality therefore, it is not physically valid. for example, considered an inductor in series with an ideal current source which is physically impossible configuration and the bond graph looks like.
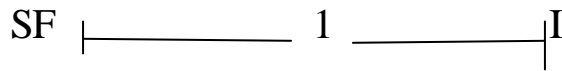
SF ——————— 1 ——————— I

Assigning causality to source bond we get ,

SF |——————— 1 ——————— I

propageting the causality through the junction will give,

SF |——————— 1 |——————— I

But assigning causality to inductor will give,

$$\text{SF} \;\vdash\!\!\!\rule{3cm}{0.4pt}\;\; 1 \;\;\rule{3cm}{0.4pt}\!\!\!\vdash \text{I}$$

the causality on the right bond is redundant therefore this is valid disability which leads to automatically identify impossible configuration is a major advantage of bond graph.

4.2 Assumptions taken during modelling through bond graph

The following assumptions are made during bond graph modelling of rotor with squeeze film damper with centralising spring :

    i.   The rotor is rigid and symmetric.

    ii.   The angular speed of rotation is constant.

    iii.   No significant exciting forces are introduced by the rolling-contact bearings.

    iv.   The oil film thickness is small compared to the radius of the journal. So, the curvature of the oil film is negligible.

    v.   The pressure gradient along the oil film thickness (in a radial direction) is small, and it is ignored.

    vi.   The velocity gradient along the oil film thickness (in a radial direction) is small, and it is ignored. In fact, the lubricant fluid flow is a two-dimensional.

    vii.   Since the lubricant fluid flow is steady, the internal forces acting on the fluid elements are ignored.

    viii.   The volume forces acting on the particles of fluid are neglected.

    ix.   It is assumed that the lubricant fluid flow is laminar.

    x.   The extent of the positive pressure region is the same for completed and ruptured   films.

    xi.   The gyroscopic effect is neglected.

    xii.   Displacement of the rotor in the axial direction is neglected.

    xiii.   The centralizing spring is considered as linear spring.

    xiv.   Excitation forces of the ball bearings are neglected.

4.3.1 Bond graph model of shaft

The shaft model is based on the Rayleigh beam model where inertia rotary inertia of the speed is included. Shaft elements with shear forces and moments acting on it can be modeled where the stiffness of the shaft elements relates the generalized Newtonian forces to generalize displacement at the ends of element. The stiffness Matrix can be modelled as a 4-port compliance field storing energy due to the four generalized displacement.
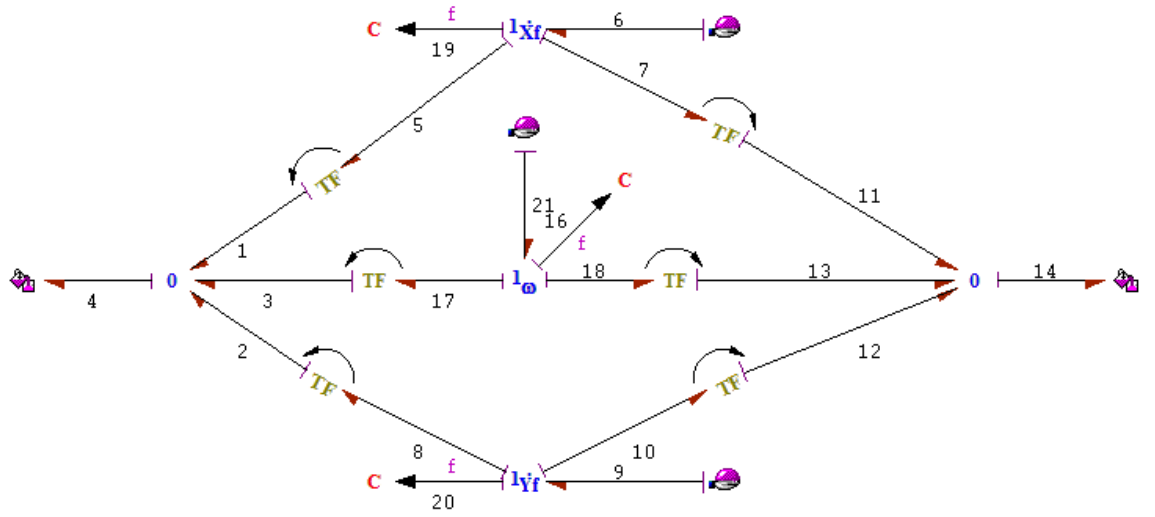

Figure 4.3 : Fixed to rotating frame velocity transformer capsule (sub system)

The fixed to rotating frame velocity Transformer capsule has been used four times to transform $\dot{X}_f, \dot{Y}_f, \dot{\omega}_f, \dot{\theta}_f$ to rotating frame to model internal damping of the shaft in rotating frame through the R- fields, which brings out the tensorial nature of the rotating internal damping. The symbol for this transfer capsule is

 . It is used in the bond graph of shaft.

The following glue ports have been used in the bond graph modelling of the components. Glue ports are the connecting link between two capsules which enables transfer of flow and effort between capsules.

 is effort input glue port .It is used to give effort into a sub model (capsule) .The effort coming from an sub system can be transfer to other sub model with the help of this glue port.

 is the flow input glue port .It is used to give flow into a sub model(capsule). The flow coming from an subsystem can be transfer to other sub model with help of this glue port.

 is the effort output glue port . It is used to take out the effort from an sub model (capsule).

 is the flow output glue port . It is used to take out the flow from an sub model (capsule).

The bond graph drawn is shown below.

In the bond graph model of shaft flow input glue port is used to give flow to shaft in two linear velocity motion in x and y and two velocity component in angular motion in $\theta \ and \ \Psi$. The output from the capsule is taken with the flow output glue port similiarly from two linear components and two angular components.
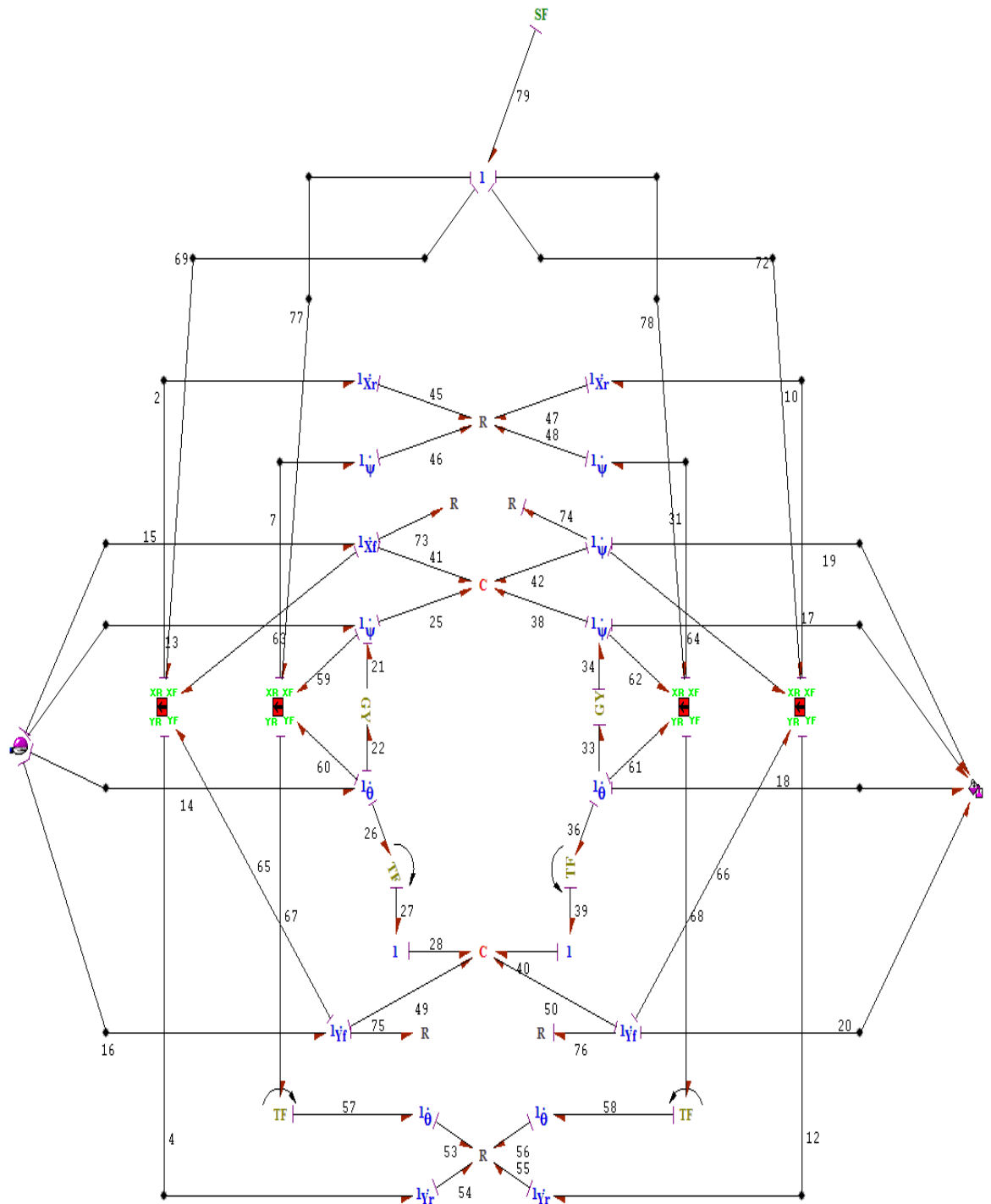
Figure 4.4 : Bond graph model of shaft

4.3.2 Bond graph model of Squeeze film damper with centralising spring having antifriction bearing

The physical configuration of squeeze film damper with centralizing spring is same as discussed in mathematical modelling chapter. In it compliance associated with various e such as stiffness of centralizing spring , stiffness of Damper housing is considered . In this model the displacement of corresponding elements such as damper housing, damping oil ,damper journal is considered in both x and y directions with both linear displacement as well as angular displacement .In the model the damping associated with different element is obtained as

Damping due to centralizing spring(R_{cs})= μ_{oil} × Stiffness of

centralizing spring (C_{cs})

 Damping due to Damping housing ($R_{dh)}$) =μ_{oil} × Stiffness of

damping housing (C_{dh})

The squeeze film damper also consist of ball bearing in the centre . In the designing of the ball bearing we have considered multibody bond graph model. In it the Contact stiffness, contact damping effects, contact slip, bearing clearance, traction between elements, rotational friction torques, and localized faults were included. While axial motion ,dynamics of cages is neglected. The bond graph drawn is shown below:

In the bond graph flow input glue port is used to give flow to the capsule. The effort is taken as ouput from two effort output glue ports.
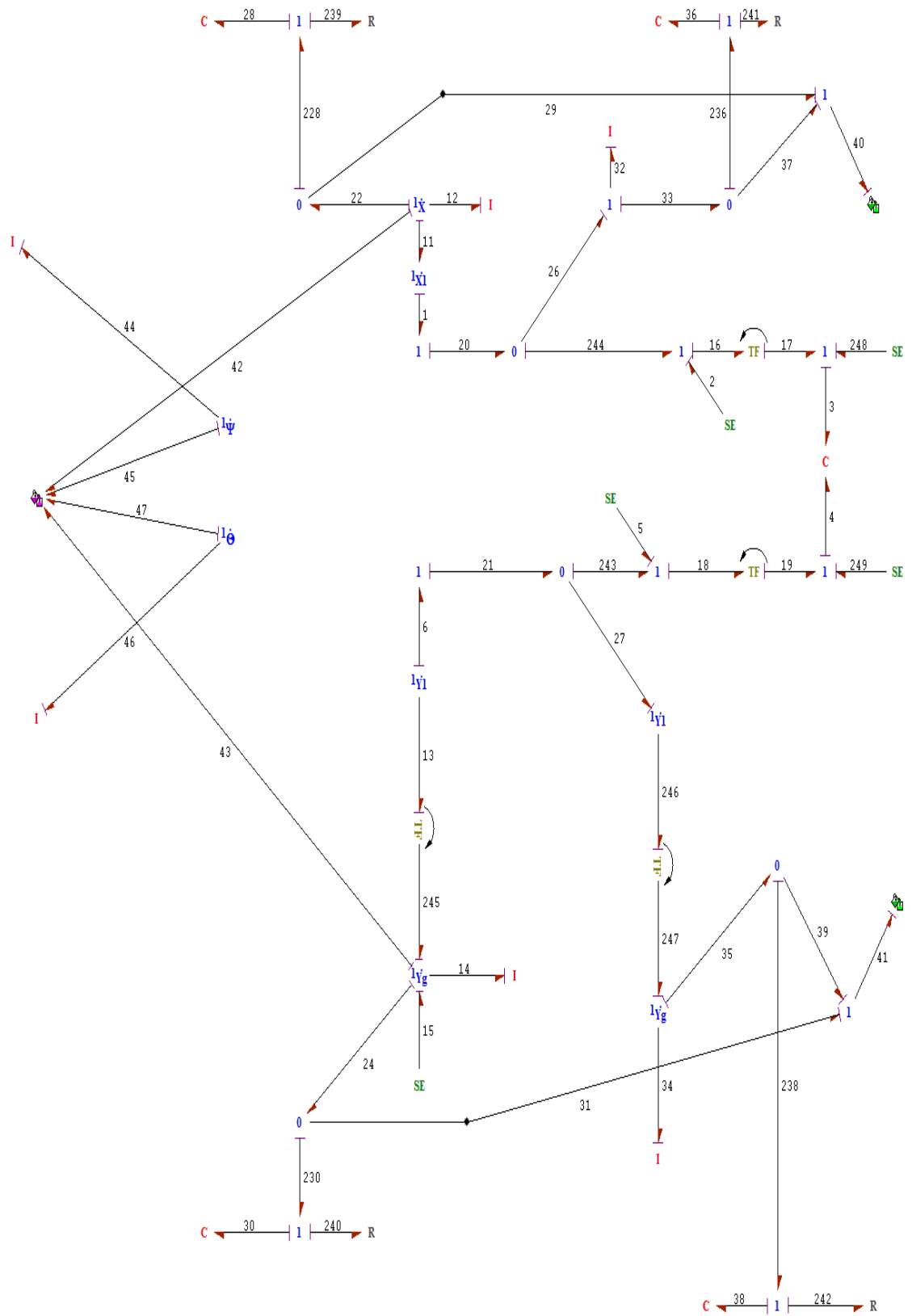
Figure 4.5: Bond graph model of squeeze film damper

4.3.3 Bond graph model of spinning hub

The spinning hub is used to model the annular disks. The model incooperates the eccentricity of hub centre of mass and its angular orientation is recorded by the flow-activated element.The expressions of the mass and the rotary inertia contribution from the interfacing shaft element are added to those of the hub.Flow activated elements records the displacement of the hub centre of mass with zero initial condition of the corresponding state vectors give the displacement of the hub axis.

In the bond graph model of spinning hub effort is taken with the help of effort glue port and the output from the capsule is in the form of flow which is taken to other capsule with the help of flow output glue port.
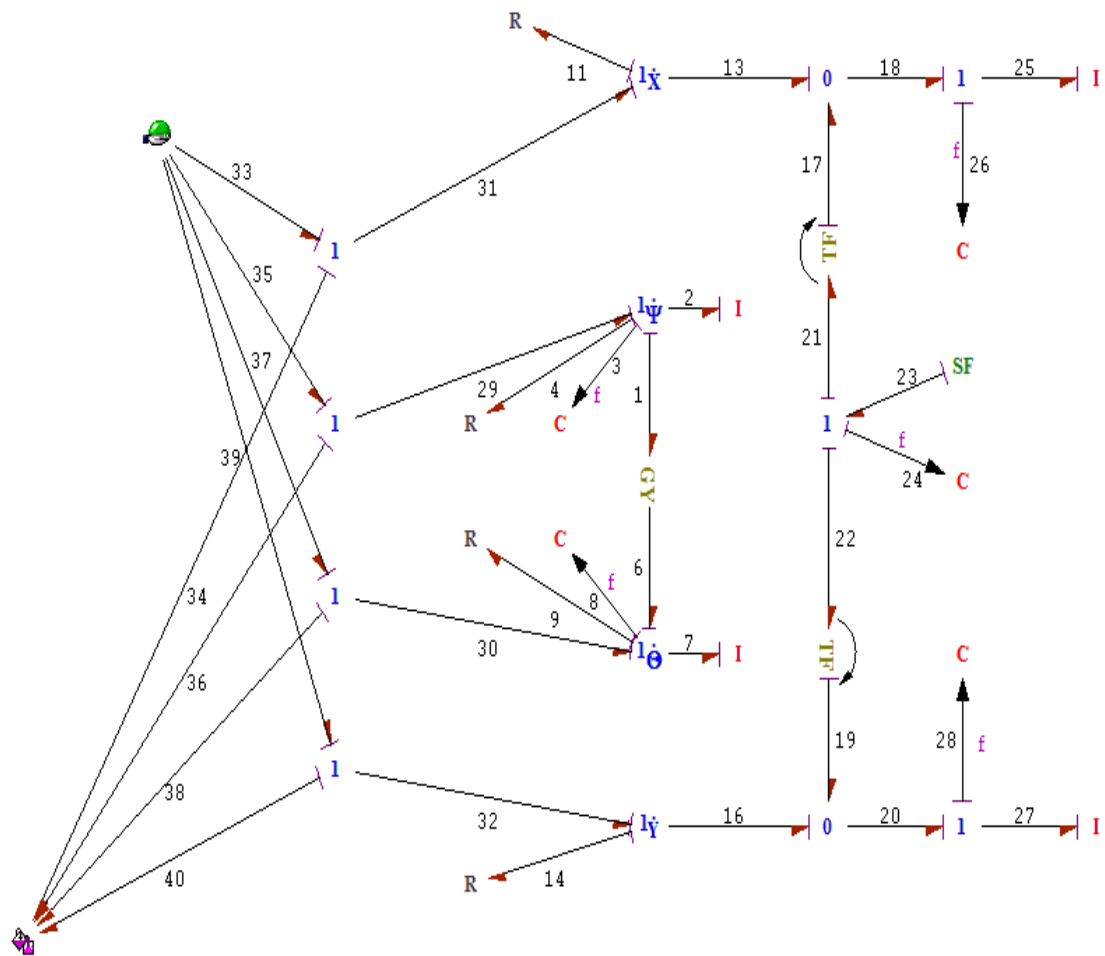
Figure4.6: Bond graph model of spinning hub

51

4.3.4 Bond graph model of ball bearing:

A deep groove ball bearing consisting of balls, inner race and outer race was modeled as a multibody system using vector bond graphs. Contact stiffness, contact damping effects, contact slip, bearing clearance, traction between elements, rotational friction torques, and localized faults were included. Axial motion, lubrication effects, structural flexibility except at contacts, and dynamics of the cage were neglected. The bond graph drawn is shown below:

In this bond graph flow is given as input in four components two in linear (x and y) and two in angular (θ and ψ) using flow input glue port and effort is taken as output using two effort output glue port.
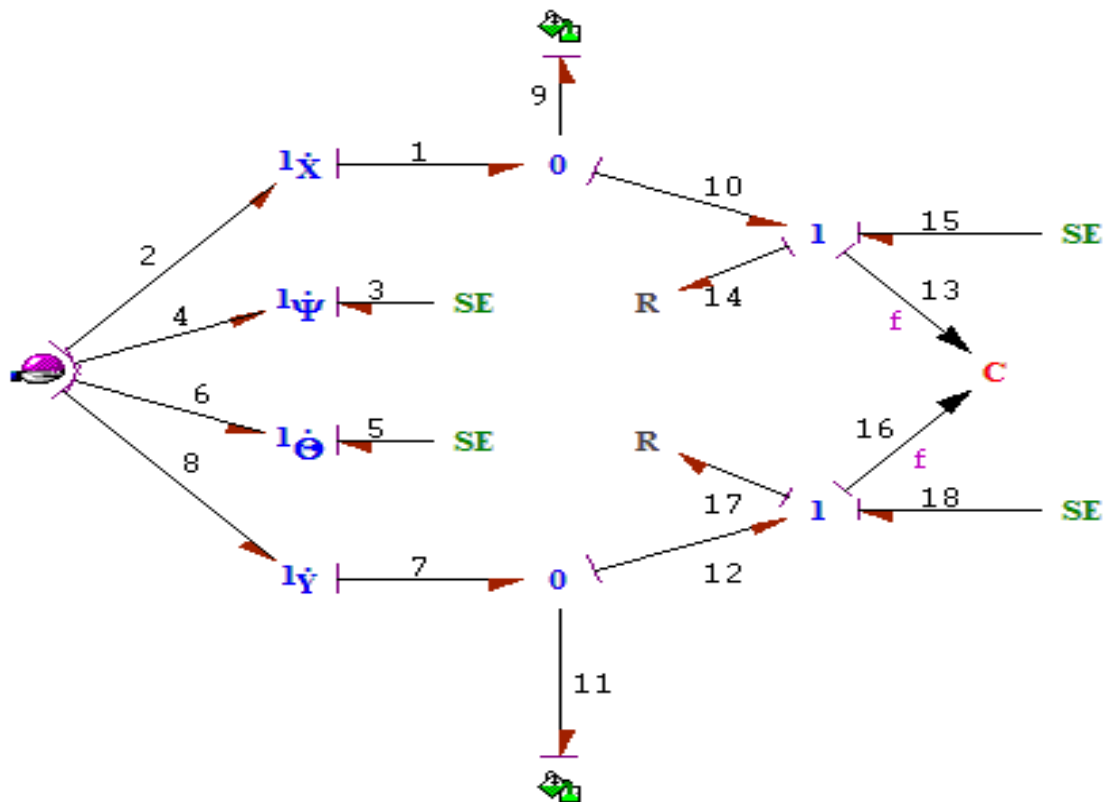
Figure 4.7: Bond graph model ball bearing

4.3.5 Bond graph model of bearing end support:

As discussed in the mathematical modelling of bearing support. In Bond graph modelling of bearing support we have considered as the end support mass as a lumped mass and as it also has stiffnesss and damping which are connected in parallel so that they have equal flow.. The bond graph drawn is shown below. In this bond graph effort is given as input using effort input glue port and effort is taken as output using effort output glue port.
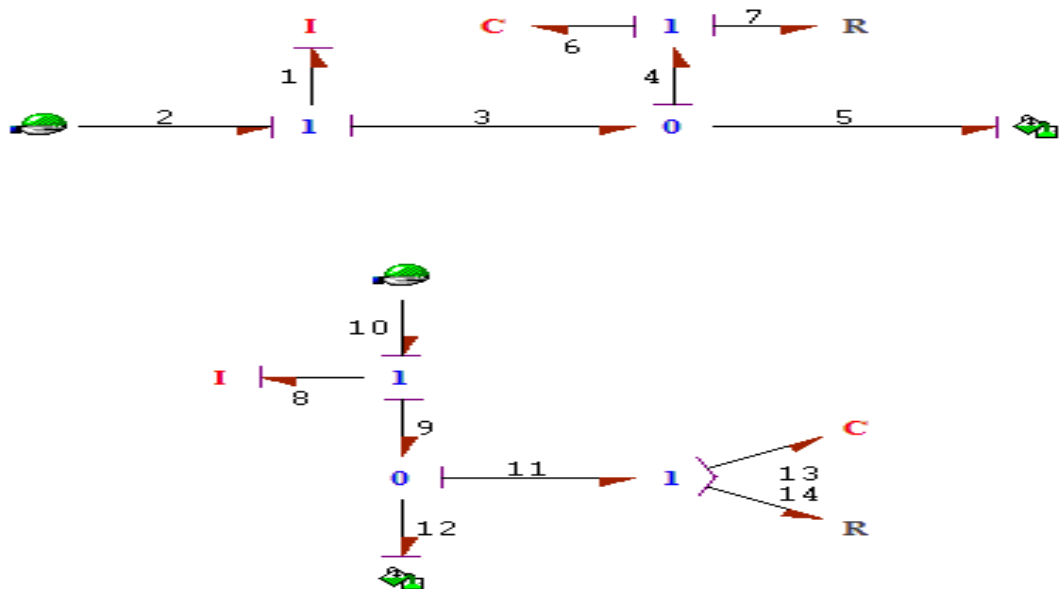

Figure 4.8: Bond graph model of bearing end support

4.4 Summary of chapter

In this chapter the bond graph model of different component is made using symbol sonata software . The bond graphs are connected to form rig in the next chapter and simulation of the rig is carried out using simulator of symbols sonata

CHAPTER -5

SIMULATION STUDY

5.1 INTRODUCTION

Computer simulation can compress the performance of a system over years into a few minutes of computer running time. Simulation models are comparatively flexible and can be modified to accommodate changing environment to real situation. There is no area, where the technique of computer simulations cannot be applied as the complexities of problem increases with the scope of application of simulation equations. At present, most of the simulation models are made by means of differential equations. In this research, analysis of rotor with squeeze film damper bearing having centralising spring is done with various parameters using bond graph and simulator of symbols- sonata software are used.

5.2 Simulation environment

This simulator of symbols Sonata, which is the based on post-processing module of SYMBOLS Sonata, is used for of rotor with squeeze film damper bearing having centralising spring is done with various parameters

SYMBOLS Sonata software

SYMBOLS Sonata is the next generation of SYMBOLS software (Symbols Modelling by Bond graph Language and Simulation) running in Microsoft Windows 95/ 98/ XP/ NT 4.0 environment. It is a modelling, simulation and control system software for a variety of scientific and Engineering applications. Being a powerful research tool, it can help avoid unaffordable, sophisticated fabrications. Yet , one may know precisely the response characteristics of the simulated system. A model in SYMBOLS sonata may be created using combination of Bond graphic elements , block diagram elements in capsulated form or other capsules. Even model can be created purely using capsules. Sub-model (capsules) can be imported from the huge capsules library or can even be created by modeller. The pre-cast capsules are not Pandora's boxes. They can be opened using Bond pad editor and customised according to the modeler's need.

Modeler may personalized and organised capsule created by them to separate their capsule group from other users.

Few features of SYMBOLS Sonata Software is as follows:

- ➢ Drawing a bond graph model.
- ➢ Augmenting the model by numbering the bonds, assigning power direction.
- ➢ Causality, module of 2- port elements, bond activation etc.
- ➢ Validation of Bond graph. Bondgraph's integrity is validated after the model is created.
- ➢ Creation of non-integrated observers in the form of detectors.
- ➢ Equations can be generated and displayed on single pallets.
- ➢ Creation of expressions.
- ➢ Generation of program code.
- ➢ Creation of sub-system models henceforth called as capsules and incorporation of capsules in a bond graph model.
- ➢ fault diagnosis.
- ➢ Preparing models for simulator and control modules.
- ➢ Export of sub system and Systems model to MATLAB/ simulink environment.
- ➢ Integrated simulation environment.
- ➢ Easy to access control panels.
- ➢ Multiple and intelligent entry mode.
- ➢ Online plotting, pause, stop and resume option.
- ➢ On line parameter variation throough slider during simulation.
- ➢ Continuous Run simulation, multiple simulations of different systems at the same time.
- ➢ Simulation extension facility.
- ➢ Advanced post simulation plotting facilities.
- ➢ Online code editing and compilation.
- ➢ Different integration methods for stiff equations.
- ➢ Multi-run facility with interpolated or discrete parameter values.

➢ Event handlers and notification messages.

➢ Direct debugging and variable tracking.

➢ Improved external date and chart interpretation routine.

➢ Export routines for Microsoft Excel database.

5.3 Simulation properties

The bond graft model of the rigid rotor with squeeze film damper is simulated for 2 seconds to obtain different output responses. Total 8194 records are used in simulation and simulation error is kept in order of 5×10^{-4} . Runge-Kutta Gill method of fifth order is used in present work to solve the differential equations generated through Bond graph model.

5.4 Ranga kutta method

Ranga kutta methods propagate a solution over an interval by combining the information from several Euler-style steps (each involving one evolution of state equations), and then using the information obtained to match a Taylor series expansion up to some higher order. This method treats every step in a sequence of steps in identical manner. This is mathematically correct, since any point along the trajectory of an ordinary Differential equation can serve as an initial point. Fifth-order Runge-Kutta method, is used in present simulation work.

5.5 Simulation Rig

In this setup , one may have ball bearing support connect at the either ends. And on one end we have ball bearing with squeeze film damper with centralising spring is connected to shaft then the shaft is connected to another shaft with the help of spinning hub and the shaft is connecting to antifriction ball bearing and to the bearing support. The experimental rig is shown in figure 5.1:
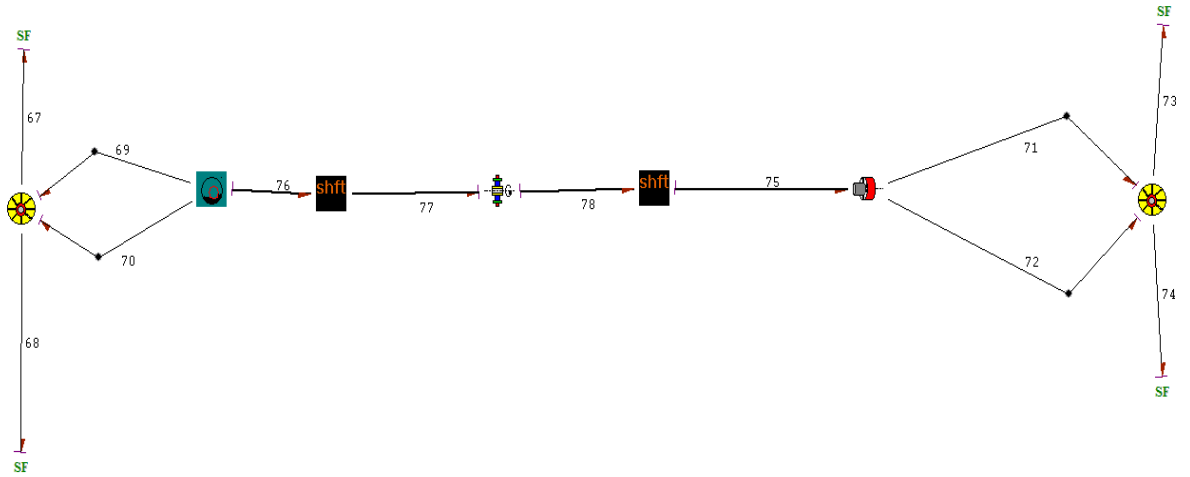
Figure 5.1: Simulation Rig

5.6 Simulation parameters
These parameters are used in the simulation of the bond graph model.

Table 5.1 : Parameter values for simulation

Parameter	Value
Bearing Support	
Mass of Hub	1kg
Dampness in X-direction	1.0Ns/m
Dampness in Y-direction	1.00Ns/m
Stiffness in X-direction	$1.00e^{6}$N/m
Stiffness in Y-direction	$1.00e^{6}$ N/m

Spinning Hub	
Angular speed	600rad/s
Material density	8000 kg/m^3
Inner radius of end of spinning hub	1x 10^{-3}m
Mass of spinning hub	0.60 kg
Eccentricity of hub	0.001 m
Rotational damping about diametrical axes	$1.25e^{-4}$ Ns/m
Rotational damping about mass centre	$1.25e^{-4}$ Ns/m
Polar moment of Inertia	0.0003675kgm^2

Shaft	
Length of shaft	0.5m
Thickness of shaft	0.0047m
Young's modulus (E)	$210.0e^9$
Outer radius of shaft	0.0048m
Inner radius of shaft	0.0001m
Material damping coefficient of shaft	2.25
Squeeze film damper	
Clearance	$50e^{-6}$
Viscosity of oil	0.02 N.s/m^2
Bearing Radius	0.01m
Bearing Length	0.01m
Mass of journal	0.10 kg
Mass of damper housing	1.00kg
Polar moment of Inertia of bearing block	0.000007696 kg/m^2
Stiffness of centralising spring	5000 N/m
Stiffness of Damper housing	$1.00e^6 \, N.s \,/m^2$
Material Damping property of centralizing spring and Damper Housing	$1.00e^{-4}$N.s/m
Initial eccentricity ratio at the time of assembly	0.01
Initial attitude angle in Rad rad	0.01
Initial squeeze Rate along the line of attitude	0.01

5.7 Summary of the chapter

In this chapter simulation software is discussed along with simulation properties and simulation rig setup is explained. The description of simulation parameters is given. With the help of given parameters the results are obtained in next chapter.

CHAPTER-6

RESULTS AND DISCUSSION

6.1 Introduction

This chapter presents the simulation results of bond graph model of rigid rotor on squeeze film damper having centralizing springs. In this one can may taken into consideration the motion of centre of mass of rigid rotor with change in various parameters.

6.2 Various variable parameters

One may changed various parameters related to squeeze film damper and observed its effect on Vibration amplitude of centre of mass of rigid rotor. The variable parameters are discussed below :

6.2.1 Angular speed

The angular speed of rotation of the rig have been changed from minimum value of zero rad/s to maximum value of 1200 rad/s. The effect of which has been observed .

Case I:

At angular speed=240 rad/s , stiffness of centralising spring =5000 N/m , Clearance =1e-3 m, viscosity of oil = 0.02 Ns/m. The following plot has been obtained between X-coordinate of centre of mass of rotor vs Y- coordinate of the centre of mass of rotor.
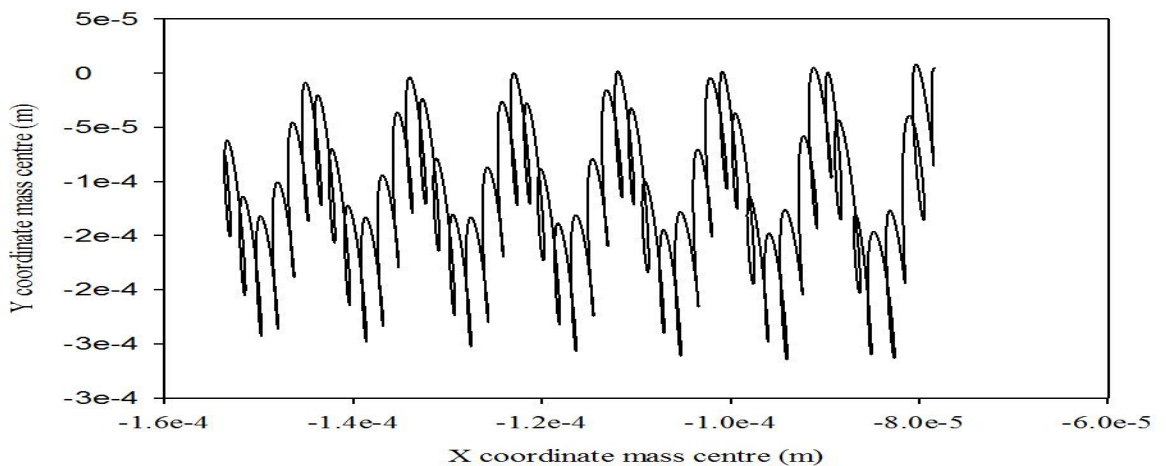
Figure 6.1 : Variation in the position of centre of mass of rotor at angular speed= 240 rad/s

Case II :

Again by changing angular speed=600 rad/s and keeping other parameter the same ,one may get following curve
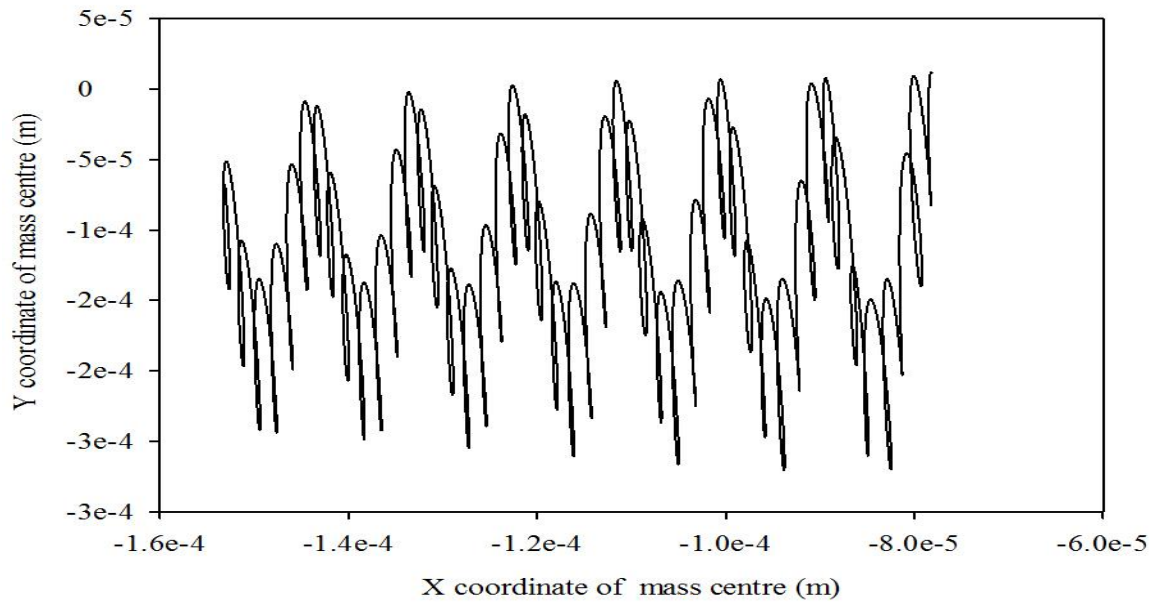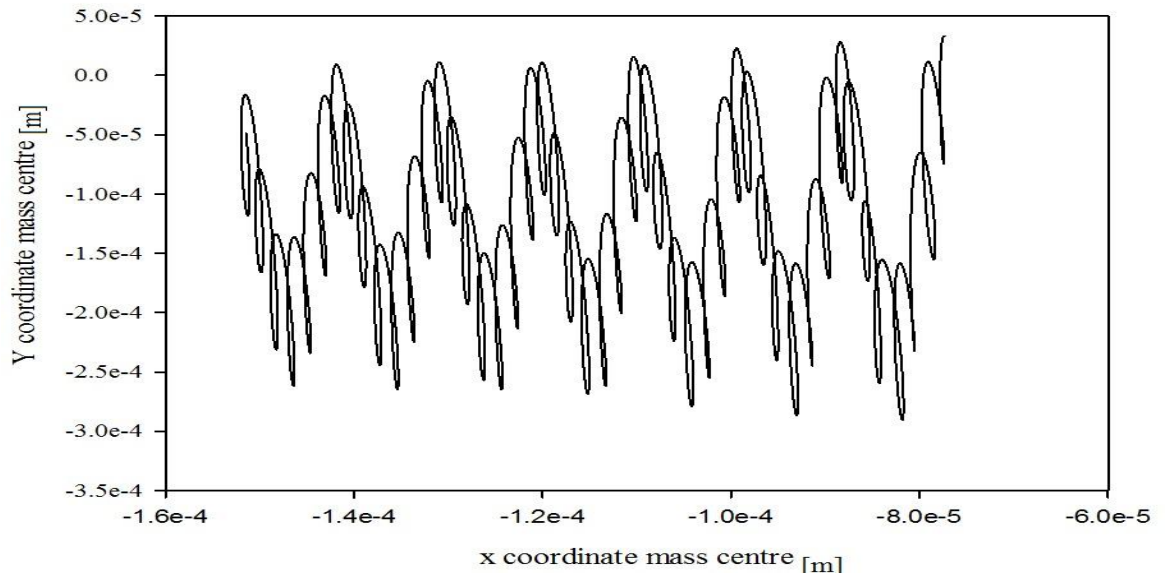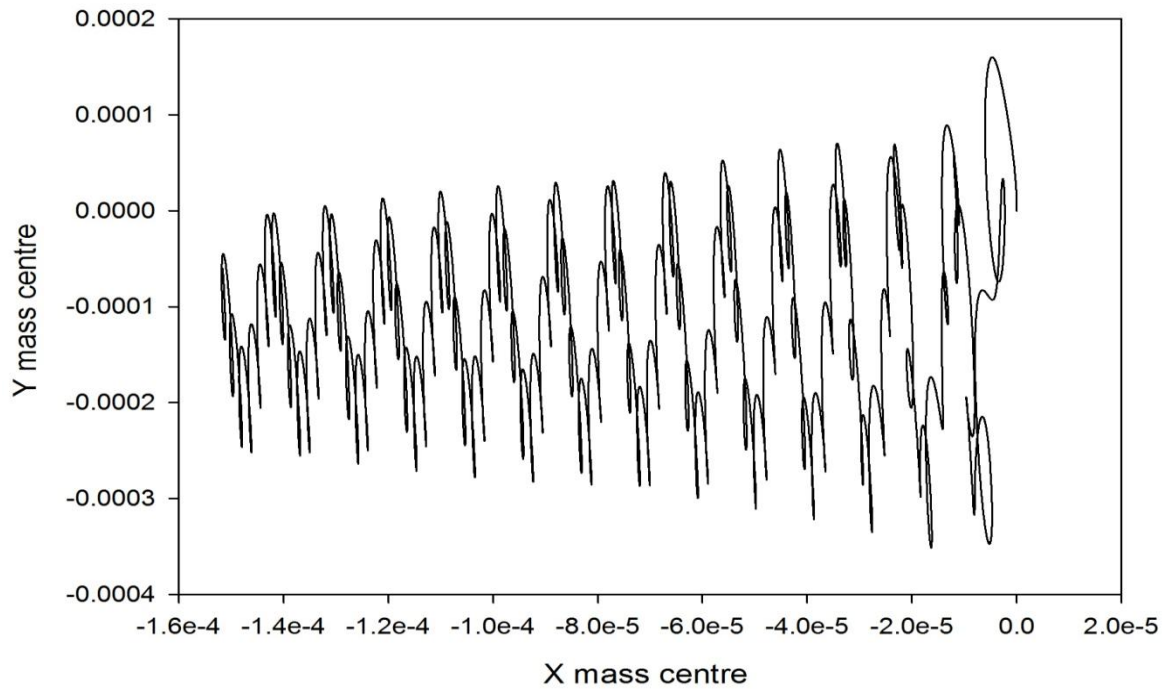

Figure 6.2 : Variation in postion of centre of mass of rotor at angular speed= 600 rad/s

Case III:

Again by changing angular speed=960 rad/s and keeping other parameter the same , one may get following curve :
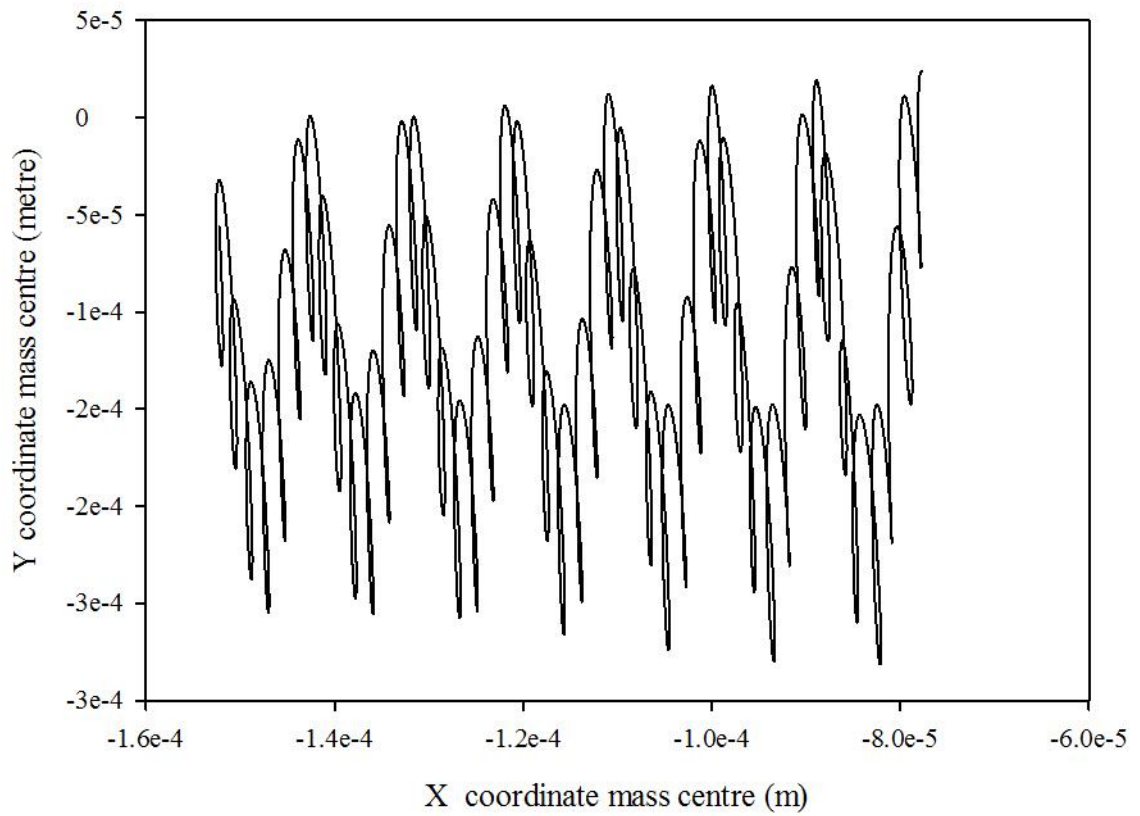
Figure 6.3 : Variation in postion of centre of mass of rotor at angular speed= 960 rad/s

Case IV:

Again by changing angular speed=1200 rad/s and keeping other parameter the same , one may get following curve:

Figure 6.4 : Variation in postion of the centre of mass of rotor at angular speed= 1200 rad/s.

From the above plots we can conclude that due to increase in speed vibration amplitude of centre of mass of rigid rotor initially increases continuously with increase in speed.

6.2.2 Bearing clearance

The bearing clearance of squeeze film damper have been changed from minimum value of $50\ e^{-6}$m to maximum value of $1000e^{-6}m$. The effect of which has been observed .For low value of bearing clearance the shaft does not rotate so the variation in the amplitude of vibration of centre of mass of rotor was not recorded but at higher clearance the following variation are observed.

Case I:

Angular speed=600 rad/s , stiffness of centralising spring =5000 N/m , Clearance =0.0008 m, viscosity of oil =0.02 Ns/m. The following graph has been obtained between X-coordinate of centre of mass of rotor vs Y- coordinate of the centre of mass of rotor.

Figure 6.5 : Variation in postion of centre of mass of rotor at Clearance =0.0008 m.

Case II:

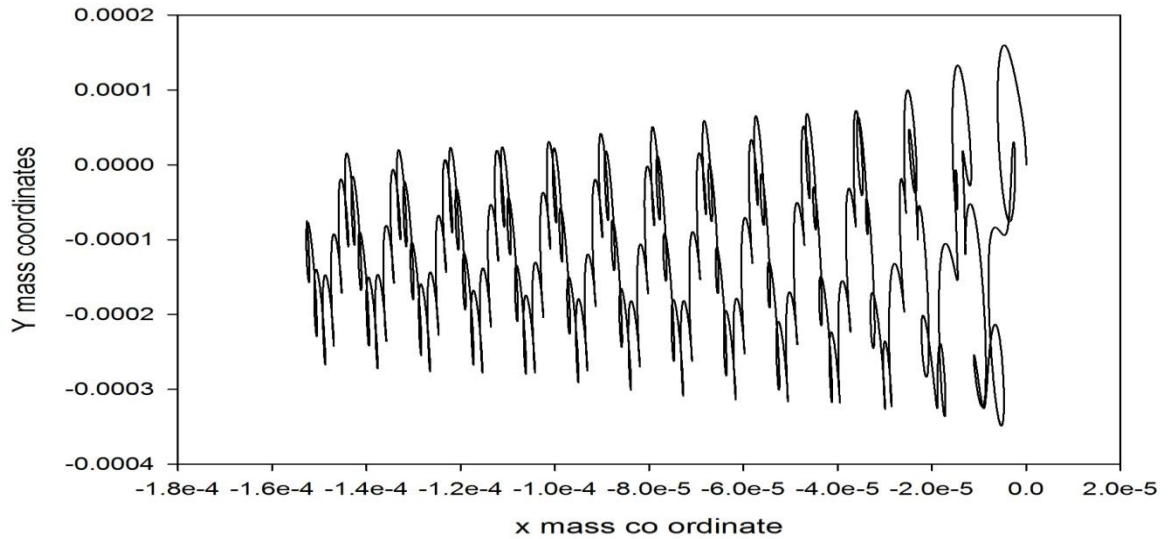Again one may increase the bearing clearance =1e-3m and keeping other parameter the same , then we get the plot as follows:

Figure 6.6 : Variation in postion of the centre of mass of rotor at Clearance =0.001 m.

For less bearing clearance system does not work in earlier stages but with 0.0008m clearance it starts working and with further increase in clearance the centre of mass of rigid starts to vibrate with more magnitude.

6.2.3 Viscosity of oil

  The Viscosity of oil of squeeze film damper have been changed from minimum value of zero N.s/m^2 and maximum value of 0.04 $N.s/m^2$. The effect of which has been observed by considering following cases.

Case I:

Angular speed=600 rad/s , stiffness of centralising spring =5000 N/m , Clearance =1e-3 m, viscosity of oil =0.008 Ns/m. The following plot has been obtained between X-coordinate of centre of mass of rotor vs Y- coordinate of the centre of mass of rotor.
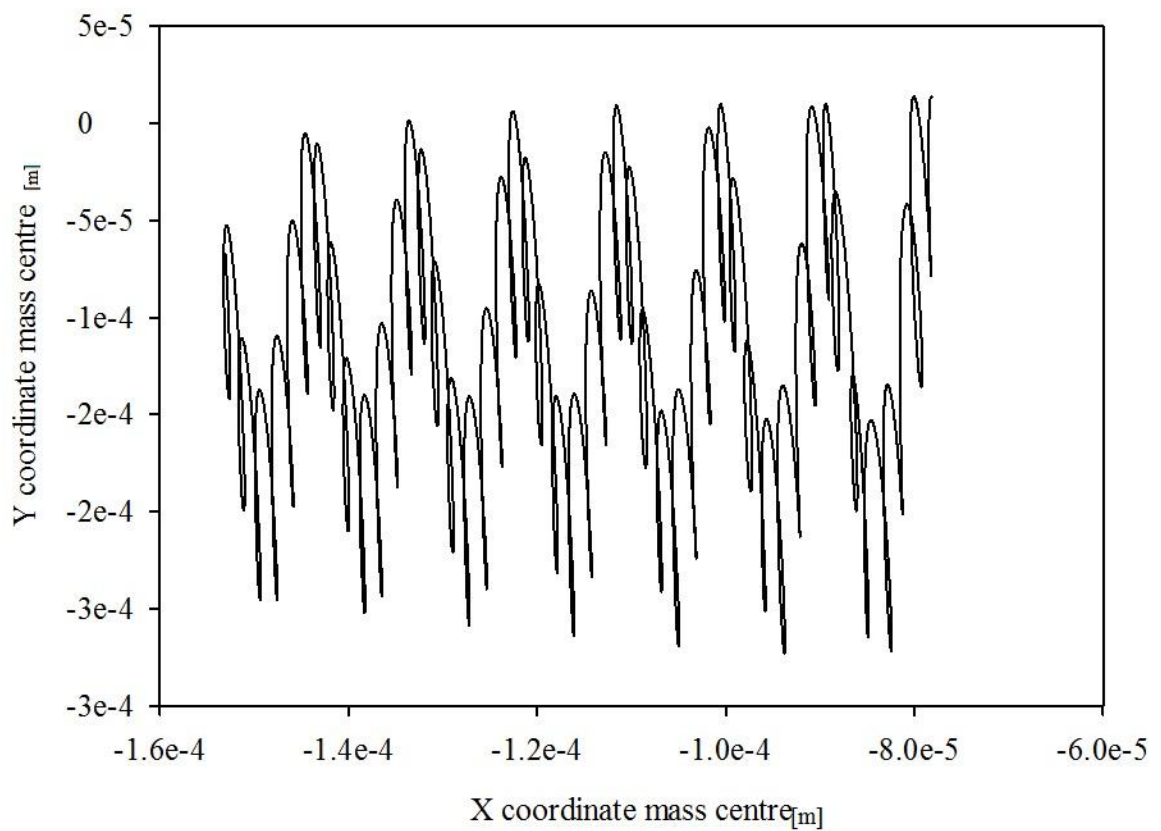
Figure 6.7 : Variation in postion of the centre of mass of rotor at viscosity of oil =0.008 Ns/m.

Case II:

Again one may increase viscosity of oil=0.02 Ns/m, and keeping other parameter same. We get the curve as follows.
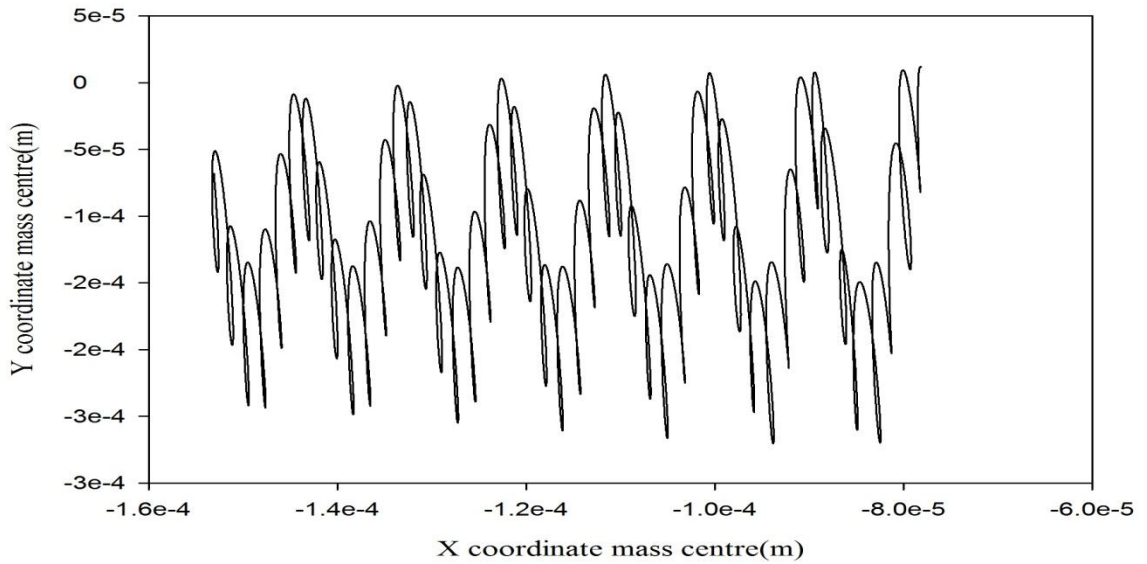
Figure 6.8 : Variation in postion of the centre of mass of rotor at viscosity of oil=0.02 Ns/m.

Case III:

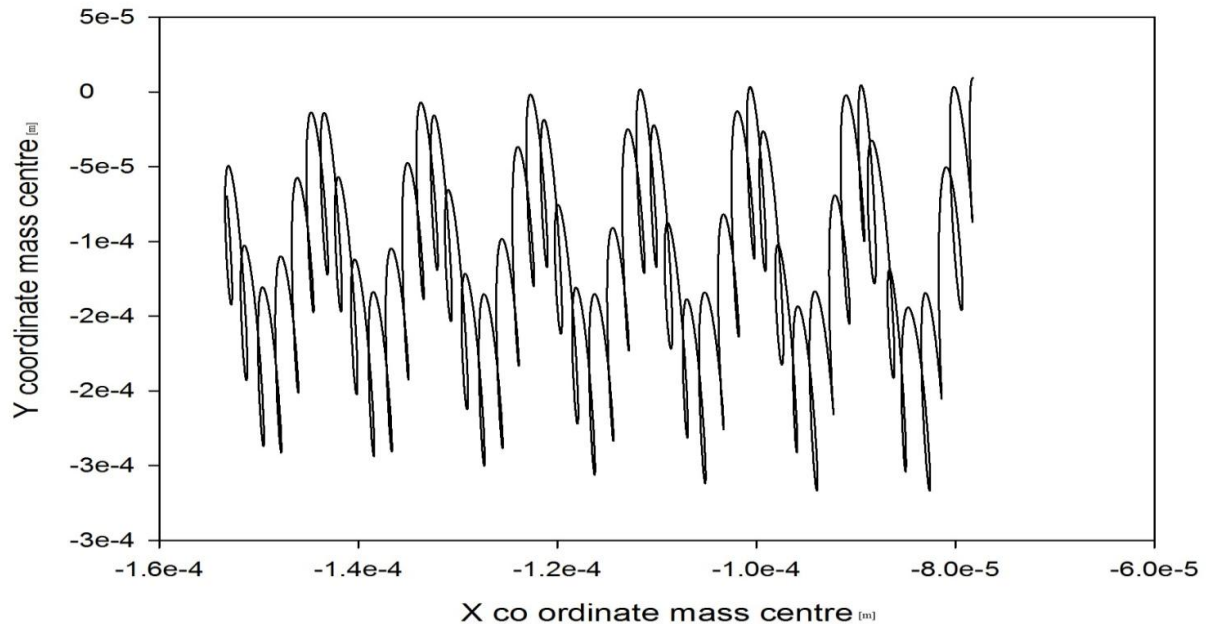Increasing the viscosity of oil =0.032 Ns/m, and keeping other parameters same , we get the curve as follows:
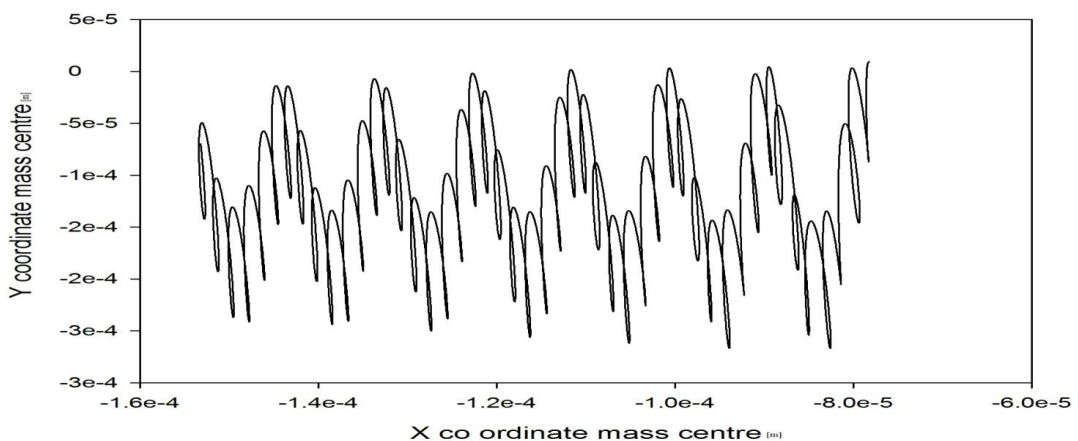
Figure 6.9 : Variation in postion of the centre of mass of rotor at viscosity of oil =0.032 Ns/m .

Case IV:

Increasing the viscosity of oil =0.04 N.s/m and keeping other parameters same , we get the graph as follows:

Figure 6.10 : Variation in postion of the the centre of mass of rotor at viscosity of oil =0.04 Ns/m .

From the above graph one may conclude that the amplitude of vibration of centre of mass of rigid rotor are decreasing continuously with increase in viscosity of the oil.

6.2.4 Stiffness of centralizing spring

 The stiffness of centralizing spring of squeeze film damper have been changed from minimum value of 5000 N/m to maximum value of $1e^5$ N/m . The effect of which has been observed in the following plots. For low value of the stiffness of centralizing spring, the shaft does not rotate so the variation in the amplitude of vibration of centre of mass of rotor was not recorded but at higher stiffness the following variation are observed.

Case I:

Angular speed=600 rad/s , stiffness of centralising spring =50000 N/m , Clearance =0.001 m, viscosity of oil =0.02 Ns/m.one may get the following.
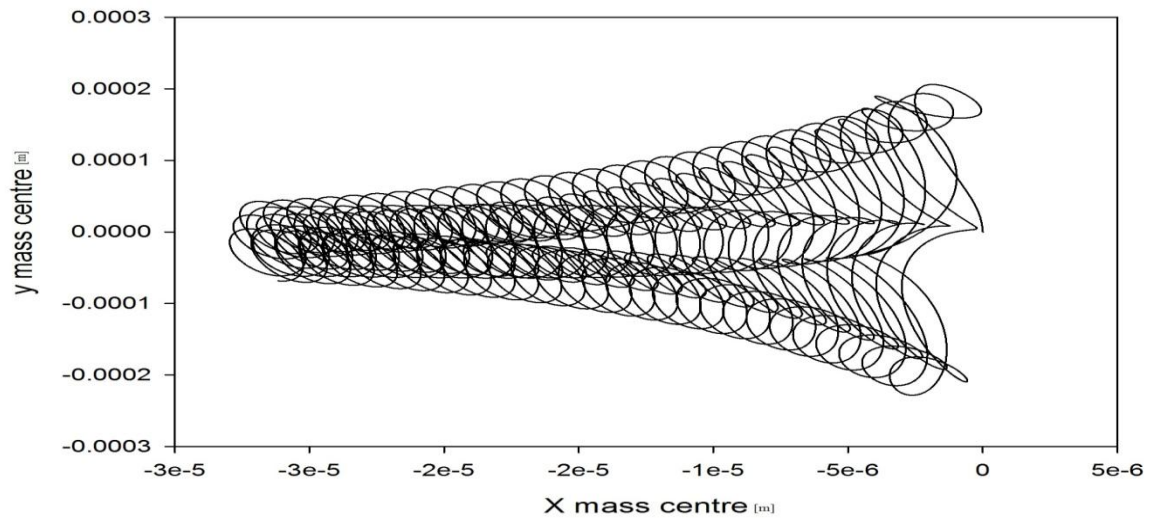

Figure 6.11 : Variation in postion of the centre of mass of rotor at , stiffness of centralising spring =50000 N/m..

Case II:

Increasing stiffness of centralising spring =80000 N/m and keeping other parameters same . one may get the plot as follows.
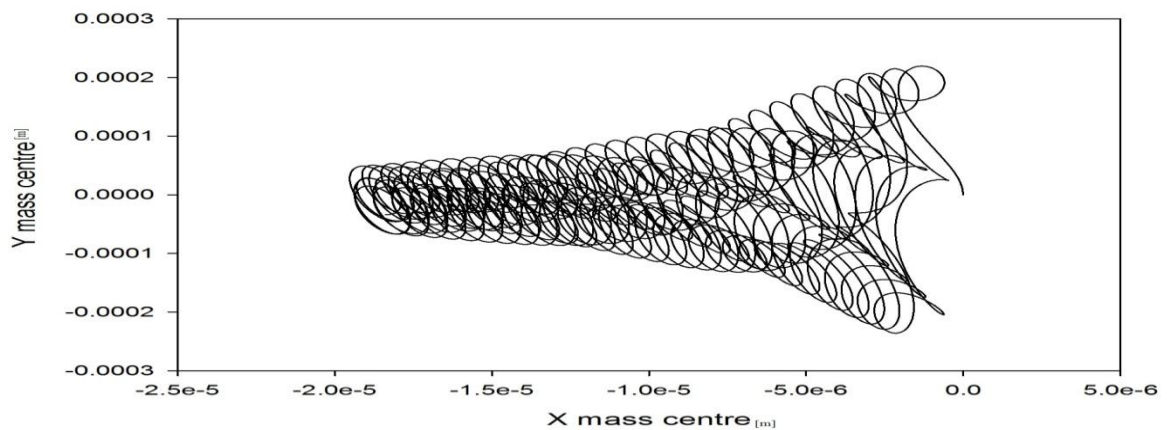

Figure 6.12 : Variation in postion of the centre of mass of rotor at , stiffness of centralising spring =80000 N/m.

For low value of stiffness in centralizing spring the system does not work as the antifriction bearing journal was in contact with outer periphery of squeeze film damper . But with the increase of stiffness the rotor starts to rotate at stiffness of

centralizing spring =50KN/m and with increase in stiffness of centralizing spring the amplitude of vibration starts decreasing.

6.3 Results and discussion

From the above graphs we can make the conclusions that

1) **Variation in speed :-**

Due to increase in speed vibration amplitude of centre of mass of rigid rotor increases continuously with speed.

This is because of the reason that due to increase in speed the magnitude of the unbalanced force increases which results in more deviation from the original position of the centre of rotor.

2) **Variation in Bearing clearance :-**

For less bearing clearance squeeze film bearing system does not work in earlier stages but with 0.0008 m clearance it starts working and with further increase in clearance the centre of mass of rigid starts to vibrate with more magnitude.

This is due to the reason that with very low clearance the motion was not possible as there was very less space for the shaft to move in the squeeze film damper. With increase in bearing clearance the vibration amplitude increases as the squeeze film damper journal gets more space to move during its motion ,as the other parameters are the same ,it increases the amplitude of vibration of the rotor.

3) **Variation in Viscosity :-**

Due to increase in viscosity the mass centre vibration decreases with increase in viscosity of oil . Due to increase in viscosity of oil ,the damping coefficient of the squeeze film damper increases which provides more damping and shock absorbing capability to the squeeze film damper. Due to increase in damping the amplitude of vibration decreases.

4) **Variation in Stiffness of Centralizing spring :-**

For low value of stiffness in centralizing spring the system does not work as the antifriction bearing journal was in contact with outer periphery of squeeze film damper . But with the increase of stiffness the rotor starts to rotate at stiffness of centralizing spring =50KN/m and with increase in stiffness of centralizing spring the amplitude of vibration starts decreasing.

This is due to the reason that at low stiffness of centralizing spring the journal of squeeze film damper is in contact with hub and the ball bearing was not able to get rotational motion . But after certain stiffness of centralizing spring the ball bearing are centrally mounted and starts rotating .With increase in stiffness of centralizing spring the damping property of the squeeze film damper increases because the centralizing spring are used to oppose any deflection from the centre position . With more stiffness the force opposing any deflection from centre position increases , so vibration amplitude decreases with increase in stiffness of centralizing spring.

6.4 Summary of chapter

In this chapter various plots are plotted by changing different parameters such as angular speed, squeeze film damper clearance, viscosity of oil of squeeze film damper and stiffness of centralizing spring are changed and their effect on the vibration amplitude of rotor is observed . The effect obtained are according to anticipation. In the next chapter the conclusion and future scope are discussed based on the result obtained.

CHAPTER 7

CONCLUSION AND FUTURE SCOPE

7.1 Conclusion

This dissertation work has been attempted to obtain the dynamic behaviour of rotor on squeeze film damper with centralizing spring through bond graph modelling and also evaluate the effect of various parameters through simulation.

The simulation study of variation in the amplitude of centre of mass of rigid rotor is done with change in various parameters such as angular speed, oil viscosity, squeeze film damper clearance and stiffness of centralizing spring.

The following conclusions can be made :

- Vibration amplitude increases with increase in speed.
- With increase in bearing clearance the vibration amplitude increases.
- With increase in viscosity of oil of squeeze film damper ,the vibration amplitude of rotor decreases.
- With increase in Stiffness in centralizing spring the vibration amplitude decreases.

7.2 Future Scope

Following future scope has been proposed for further analysis.

- In this model only the vibration amplitude of the centre mass of rotor has been investigated.
- The forces experienced by the centre of mass due to vibration may also be considered in future .
- In present work ,only effect of serval parameters are considered , further investigation with varying some other parameters also be done.
- Same experimental rig can be made to validate the results.

REFERENCES

[1] Modaresahmadi S. ,Ghazavi M. , and SheikhzadSaravani M. (2015), " Dynamic Analysis of a Rotor Supported on Ball Bearings with Waviness and Centralizing Springs and Squeeze Film Dampers" ,IJE TRANSACTIONS C: Aspects Vol. 28, No. 9, 1351-1358.

[2] Venkata Narayana B., Diwakar Reddy V., and Krishnaiah G. (2015), " Characteristics Investigation of Squeeze Film Damper using Triangular Element", International Journal of Innovations in Engineering and Technology (IJIET), volume 5, Issue 2.

[3] Mohan S. and Hann E. J., (1974), "Design of Squeeze Film Damper Supports for Rigid Rotors", Transactions of the ASME.

[4]. Zhu C. S, Robb D. A. and Ewins D. J. (2002) , "Analysis of the multiple-solution response of a flexible rotor supported on non-linear Squeeze film dampers", Journal of Sound and vibration 252(3), 389-408.

[5] Khalid Asad A., Albagul A., Faris W. and Ismail Godem A. (2006), "An experimental study on steel and Teflon squeeze film dampers", Shock and Vibration 13, 33–40.

[6] Bouzidane A. and Thomas M. (2013), "Nonlinear Dynamic Analysis of a Rigid Rotor Supported by a Three-Pad Hydrostatic Squeeze Film Dampers", Tribology Transactions, 56:5, 717-727.

[7] Borutzky W. (2009), "Bond graph modelling and simulation of multidisciplinary systems – An introduction" , Simulation Modelling Practice and Theory 17, 3–21.

[8] Kumar H.N Ajay, D.J Shilpashree, Adarsh M.S , Amith D and Kulkarni Sadanand (2016), "Development of Smart Squeeze Film Dampers for Small Rotors", Procedia Engineering 144 , 790 – 800.

[9] Farisa Waleed F. , Khalid Asad A., Albagul A. and Ismail Godem A. (2008) " Experimental investigation of the dynamic response of squeeze film dampers made of steel and glass/epoxy", Shock and Vibration 15 , 631–637.

 [10] Cao Jianming , Dimond Timothy and Allaire Paul (2014) ,"Numerical analysis of flexible rotor with nonlinear bearings and squeeze film dampers" , IMECE2014-37365.

[11] Dousti Saeid, Gerami Ali, and Dousti Majid (2006), "A Numerical CFD Analysis on Supply Groove Effects in High Pressure, Open End Squeeze Film Dampers", International Journal of Engineering Innovation & Research ,Volume 5, Issue 1.

[12] Rodrigues Fabiano A. , Thouverez Fabrice and Jezequel Louis (2004), "Interaction of Squeeze Film Dampers and Hole Feed Systems and Its Influence on the Dynamicsof a Jeffcott Rotor" , International Journal of Rotating Machinery, 10(3): 163–174.

[13]Bouzidane A., Thomas M. and Lakis A. A. (2008), "Nonlinear Dynamic Behavior of a Rigid Rotor Supported by Hydrostatic Squeeze Film Dampers", Journal of Tribology, Vol 130.

[14] moraru Laurentiu (2014), "On the design of squeeze film dampers operating within the limits of the Reynolds theory", INCAS BULLETIN, Volume 6, Issue 4, pp. 75 – 80.

[15]Lin Jaw Ren (1997), "On Squeeze film characteristics of long partial journal bearing lubricated with couple stress fluid", Tribology International, Volume 30 Number 1 .

[16] Guo Zenglin, Hirano Toshio and Kirk R. Gordon (2003), "application of cfd analysis for rotating machinery, part 1: hydrodynamic, hydrostatic bearings and squeeze film damper" , Proceedings of ASME Turbo Expo 2003.

[17] Salbu E. O. J. (1964), "Compressible Squeeze Films and squeeze bearing", Journal of Basic Engineering.

18] Proctor Margaret P. and Gunter Edgar J. (2005) "Nonlinear Whirl Response of a High-Speed Seal Test Rotor With Marginal and Extended Squeeze-Film Dampers", NASA/TM—213808.

[19] Gunter Edgar J. and Proctor Margaret P. (2007), "Whirl motion of a seal test rig with squeeze-film dampers", vibration institute 31st annual meeting .

[20]Shende R.W. and Sane S.K. (1988) , "Squeeze Film Damping for Aircraft Gas Turbines". Def Sci J Vol38, No. 4 , pp 439-456 .

[21]Heidari Hamidreza , Ashkooh Mohammadreza (2016), "The influence of asymmetry in centralizing spring of squeeze film damper on stability and bifurcation of Rigid rotor response", Alexandria Engineering Journal.

[22]http://www.globalspec.com/learnmore/mechanical_components/bearings_bushings/radial_ball_bearings.

 [23] Internet http://www.machinedesign.com/whats-difference-between/what-s-difference-between-bearings-1.

 [24]Das Subrata and Kumar Guha Sisir (2013), "On the Steady-State Performance Characteristics of Finite Hydrodynamic Journal Bearing under Micro-Polar Lubrication with Turbulent Effect"   International Journal of Mechanical, Aerospace, Industrial and Mechatronics Engineering Vol:7, No:4.

[25] Qiang He, Lili Li, Fengzhang Ren and Alex Volinsky (2016), "Numerical Simulation and Experimental Study of the Hydrostatic Spindle with Orifice Restrictors", The Open Mechanical Engineering Journal, Volume 10.

APPENDIX A

Various expressions used in Simulation

Variable	Assignment
RIGHTEN1_Preload (double)	
BEARING1_MassSpprt_Hub (double)	
BEARING1_Suprt_DmpX (double)	
BEARING1_Suprt_StiffX (double)	
BEARING1_Suprt_StiffY (double)	
BEARING1_Suprt_DmpY (double)	
C (double)	
FINITES1_C (double) : Bearing Clearance	FINITES1_C=C;
MU (double)	
FINITES1_MU (double) : Viscosity of oil	FINITES1_MU=MU;
R1 (double)	
FINITES1_R (double) : Bearing radius	FINITES1_R=R1;
L (double)	
FINITES1_B (double) : Bearing length	FINITES1_B=L;
W (double)	
FINITES1_Mass (double) : Journal mass	FINITES1_Mass=W;
WH (double)	
FINITES1_MassDmpHsng (double) : Mass of Damper Housing	FINITES1_MassDmpHsng=WH;
Ip (double)	
FINITES1_Ibpolar (double) : Polar MI of Bearing Block	FINITES1_Ibpolar=Ip;
g (double)	
FINITES1_g (double) : Acceleration due to gravity	FINITES1_g=g;
Kcs (double)	
FINITES1_StfCntrSpr (double) : Stiffness of Centralising Spring	FINITES1_StfCntrSpr=Kcs;

Kdh (double)	
FINITES1_StfDmpHsng (double) : Stiffness of Damper Housing	FINITES1_StfDmpHsng=Kdh;
Mu0 (double)	
FINITES1_Mu0 (double) : Mu0 for CntrSpr and DmpHsng Damping	FINITES1_Mu0=Mu0;
FINITES1_Inisfd (int) : To initiate SFD give 1 (int)	
FINITES1_IniEPS (double) : Initial eccentricity ratio at the time of assembly	
Phai (double)	
FINITES1_Iniattang (double) : Initial Attitude Angle in Rad	FINITES1_Iniattang=Phai;
FINITES1_Inisqzrate (double) : Initial Squeeze Rate along the line of attitude	
BEARING2_MassSpprt_Hub (double)	
BEARING2_Suprt_DmpX (double)	
Ks1 (double)	
BEARING2_Suprt_StiffX (double)	BEARING2_Suprt_StiffX=Ks1;
Ks2 (double)	
BEARING2_Suprt_StiffY (double)	BEARING2_Suprt_StiffY=Ks2;
Kd (double)	
BEARING2_Suprt_DmpY (double)	BEARING2_Suprt_DmpY=Kd;
omega (double)	
SPINNIN1_AngSpeed (double) : Angular Speed rad/s	SPINNIN1_AngSpeed=omega;
Rho (double)	
SPINNIN1_Rho (double) : Material Density	SPINNIN1_Rho=Rho;
Ri (double)	

SPINNIN1_Th_next (double)	
SPINNIN1_Th_Next (double) : Thickness of Next Int. face Shaft (Zero if non-existant)	SPINNIN1_Th_next=Th;
SPINNIN1_MconPrv (double)	
SPINNIN1_MiconPrv (double)	
SPINNIN1_MconNext (double)	
SPINNIN1_MiconNext (double)	
SPINNIN1_HubMass (double)	
SPINNIN1_Ecc (double) : Eccentricity of the Hub	
SPINNIN1_AnglEcc (double) : Angle of Eccentricity from X Axis(vertical) in Degrees.	
SPINNIN1_RotDmp (double) : Rotational Damping about diametrical axes	SPINNIN1_RotDmp=1.25e-4;
SPINNIN1_TransDmp (double) : Translational Damping of Mass centre	
SPINNIN1_HubPolMI (double)	SPINNIN1_HubPolMI=0.0003675;
SPINNIN1_SF41 (double)	
shaft11_Fixedto1_AngSpeed (double) : Angular speed of the rotating frame	shaft11_Fixedto1_AngSpeed=600;
shaft11_Fixedto2_AngSpeed (double) : Angular speed of the rotating frame	shaft11_Fixedto2_AngSpeed=600;
shaft11_Fixedto4_AngSpeed (double) : Angular speed of the rotating frame	shaft11_Fixedto4_AngSpeed=600;
shaft11_Fixedto3_AngSpeed (double) : Angular speed of the rotating frame	shaft11_Fixedto3_AngSpeed=600;
shaft11_Gyrator1 (double)	
shaft11_trans26 (double)	
shaft11_Gyrator2 (double)	
shaft11_trans36 (double)	

E (double)	
shaft1_E (double) : Young's modulus	shaft1_E=E;
shaft1_Ro (double)	shaft1_Ro=Ro;
shaft1_Ri (double)	shaft1_Ri=Ri;
pi (double)	pi=3.141592653;
shaft1_pi (double)	shaft1_pi=pi;
shaft1_I (double) : second moment of area about diameter	shaft1_I=shaft1_pi*(shaft1_Ro*shaft1_Ro*shaft1_Ro*shaft1_Ro-shaft1_Ri*shaft1_Ri*shaft1_Ri*shaft1_Ri)*0.25;
shaft11_K41_41 (double)	shaft1_Lt=shaft1_L_this; shaft1_Coef=shaft1_E*shaft1_I/(shaft1_Lt*shaft1_Lt*shaft1_Lt); shaft11_K41_41=12*shaft1_Coef;
shaft11_K41_42 (double)	shaft11_K41_42=6*shaft1_Lt*shaft1_Coef;
shaft11_K41_25 (double)	shaft11_K41_25=-shaft11_K41_41;
shaft11_K41_38 (double)	shaft11_K41_38=shaft11_K41_42;
shaft11_K42_41 (double)	shaft11_K42_41=shaft11_K41_42;
shaft11_K42_42 (double)	shaft11_K42_42=4*shaft1_Lt*shaft1_Lt*shaft1_Coef;
shaft11_K42_25 (double)	shaft11_K42_25=-shaft11_K41_42;
shaft11_K42_38 (double)	shaft11_K42_38=2*shaft1_Lt*shaft1_Lt*shaft1_Coef;
shaft11_K25_41 (double)	shaft11_K25_41=-shaft11_K41_41;
shaft11_K25_42 (double)	shaft11_K25_42=-shaft11_K41_42;
shaft11_K25_25 (double)	shaft11_K25_25=shaft11_K41_41;
shaft11_K25_38 (double)	shaft11_K25_38=-shaft11_K41_42;
shaft11_K38_41 (double)	shaft11_K38_41=shaft11_K41_42;
shaft11_K38_42 (double)	shaft11_K38_42=shaft11_K42_38;
shaft11_K38_25 (double)	shaft11_K38_25=-shaft11_K41_42;
shaft11_K38_38 (double)	shaft11_K38_38=shaft11_K42_42;
shaft1_Mu0 (double)	shaft1_Mu0=Mu0;
shaft11_R45_45 (double)	shaft11_R45_45=shaft1_Mu0*shaft11_K41_41;

shaft11_R47_46 (double)	shaft11_R47_46=shaft11_R46_47;
shaft11_R47_47 (double)	shaft11_R47_47=shaft11_R45_45;
shaft11_R47_48 (double)	shaft11_R47_48=shaft11_R47_46;
shaft11_R48_45 (double)	shaft11_R48_45=shaft11_R45_46;
shaft11_R48_46 (double)	shaft11_R48_46=shaft11_R46_48;
shaft11_R48_47 (double)	shaft11_R48_47=shaft11_R47_45;
shaft11_R48_48 (double)	shaft11_R48_48=shaft11_R46_46;
shaft11_K28_28 (double)	shaft11_K28_28=shaft11_K41_41;
shaft11_K28_40 (double)	shaft11_K28_40=shaft11_K41_42;
shaft11_K28_49 (double)	shaft11_K28_49=shaft11_K41_25;
shaft11_K28_50 (double)	shaft11_K28_50=shaft11_K41_38;
shaft11_K40_28 (double)	shaft11_K40_28=shaft11_K42_41;
shaft11_K40_40 (double)	shaft11_K40_40=shaft11_K42_42;
shaft11_K40_49 (double)	shaft11_K40_49=shaft11_K42_25;
shaft11_K40_50 (double)	shaft11_K40_50=shaft11_K42_38;
shaft11_K49_28 (double)	shaft11_K49_28=shaft11_K25_41;
shaft11_K49_40 (double)	shaft11_K49_40=shaft11_K25_42;
shaft11_K49_49 (double)	shaft11_K49_49=shaft11_K25_25;
shaft11_K49_50 (double)	shaft11_K49_50=shaft11_K25_38;
shaft11_K50_28 (double)	shaft11_K50_28=shaft11_K38_41;
shaft11_K50_40 (double)	shaft11_K50_40=shaft11_K38_42;
shaft11_K50_49 (double)	shaft11_K50_49=shaft11_K38_25;
shaft11_K50_50 (double)	shaft11_K50_50=shaft11_K38_38;
shaft11_R53_53 (double)	shaft11_R53_53=shaft11_R45_45;
shaft11_R53_54 (double)	shaft11_R53_54=shaft11_R45_46;
shaft11_R53_55 (double)	shaft11_R53_55=shaft11_R45_47;
shaft11_R53_56 (double)	shaft11_R53_56=shaft11_R45_48;

shaft11_R53_55 (double)	shaft11_R53_55=shaft11_R45_47;
shaft11_R53_56 (double)	shaft11_R53_56=shaft11_R45_48;
shaft11_R54_53 (double)	shaft11_R54_53=shaft11_R46_45;
shaft11_R54_54 (double)	shaft11_R54_54=shaft11_R46_46;
shaft11_R54_55 (double)	shaft11_R54_55=shaft11_R46_47;
shaft11_R54_56 (double)	shaft11_R54_56=shaft11_R46_48;
shaft11_R55_53 (double)	shaft11_R55_53=shaft11_R47_45;
shaft11_R55_54 (double)	shaft11_R55_54=shaft11_R47_46;
shaft11_R55_55 (double)	shaft11_R55_55=shaft11_R47_47;
shaft11_R55_56 (double)	shaft11_R55_56=shaft11_R47_48;
shaft11_R56_53 (double)	shaft11_R56_53=shaft11_R48_45;
shaft11_R56_54 (double)	shaft11_R56_54=shaft11_R48_46;
shaft11_R56_55 (double)	shaft11_R56_55=shaft11_R48_47;
shaft11_R56_56 (double)	shaft11_R56_56=shaft11_R48_48;
shaft11_TF_yr (double)	
shaft11_Tf_yr2 (double)	
shaft11_R73 (double)	
shaft11_R74 (double)	
shaft11_R75 (double)	
shaft11_R76 (double)	
shaft11_SF79 (double)	
shaft21_Fixedto1_AngSpeed (double) : Angular speed of the rotating frame	shaft21_Fixedto1_AngSpeed=600;
shaft21_Fixedto2_AngSpeed (double) : Angular speed of the rotating frame	shaft21_Fixedto2_AngSpeed=600;
shaft21_Fixedto4_AngSpeed (double) : Angular speed of the rotating frame	shaft21_Fixedto4_AngSpeed=600;
shaft21_Fixedto3_AngSpeed (double) : Angular speed of the rotating frame	shaft21_Fixedto3_AngSpeed=600;

shaft21_K41_42 (double)	shaft21_K41_42=6*shaft21_Lt*shaft21_Coef;
shaft21_K41_25 (double)	shaft21_K41_25=-shaft21_K41_41;
shaft21_K41_38 (double)	shaft21_K41_38=shaft21_K41_42;
shaft21_K42_41 (double)	shaft21_K42_41=shaft21_K41_42;
shaft21_K42_42 (double)	shaft21_K42_42=4*shaft21_Lt*shaft21_Lt*shaft21_Coef;
shaft21_K42_25 (double)	shaft21_K42_25=-shaft21_K41_42;
shaft21_K42_38 (double)	shaft21_K42_38=2*shaft21_Lt*shaft21_Lt*shaft21_Coef;
shaft21_K25_41 (double)	shaft21_K25_41=-shaft21_K41_41;
shaft21_K25_42 (double)	shaft21_K25_42=-shaft21_K41_42;
shaft21_K25_25 (double)	shaft21_K25_25=shaft21_K41_41;
shaft21_K25_38 (double)	shaft21_K25_38=shaft21_K25_42;
shaft21_K38_41 (double)	shaft21_K38_41=shaft21_K41_42;
shaft21_K38_42 (double)	shaft21_K38_42=shaft21_K42_38;
shaft21_K38_25 (double)	shaft21_K38_25=shaft21_K42_25;
shaft21_K38_38 (double)	shaft21_K38_38=shaft21_K42_42;
shaft21_Mu0 (double)	shaft21_Mu0=Mu0;
shaft21_R45_45 (double)	shaft21_R45_45=shaft21_Mu0*shaft21_K41_41;
shaft21_R45_46 (double)	shaft21_R45_46=shaft21_Mu0*shaft21_K41_42;
shaft21_R45_47 (double)	shaft21_R45_47=shaft21_Mu0*shaft21_K41_25;
shaft21_R45_48 (double)	shaft21_R45_48=shaft21_Mu0*shaft21_K41_38;
shaft21_R46_45 (double)	shaft21_R46_45=shaft21_R45_46;
shaft21_R46_46 (double)	shaft21_R46_46=shaft21_Mu0*shaft21_K42_42;
shaft21_R46_47 (double)	shaft21_R46_47=shaft21_K42_25;
shaft21_R46_48 (double)	shaft21_R46_48=shaft21_Mu0*shaft21_K42_38;
shaft21_R47_45 (double)	shaft21_R47_45=shaft21_R45_47;
shaft21_R47_46 (double)	shaft21_R47_46=shaft21_R46_47;
shaft21_R47_47 (double)	shaft21_R47_47=shaft21_R45_45;

shaft21_R47_48 (double)	shaft21_R47_48=shaft21_R47_46;
shaft21_R48_45 (double)	shaft21_R48_45=shaft21_R45_46;
shaft21_R48_46 (double)	shaft21_R48_46=shaft21_R46_48;
shaft21_R48_47 (double)	shaft21_R48_47=shaft21_R47_48;
shaft21_R48_48 (double)	shaft21_R48_48=shaft21_R46_46;
shaft21_K28_28 (double)	shaft21_K28_28=shaft21_K41_41;
shaft21_K28_40 (double)	shaft21_K28_40=shaft21_K41_42;
shaft21_K28_49 (double)	shaft21_K28_49=shaft21_K41_25;
shaft21_K28_50 (double)	shaft21_K28_50=shaft21_K41_38;
shaft21_K40_28 (double)	shaft21_K40_28=shaft21_K42_41;
shaft21_K40_40 (double)	shaft21_K40_40=shaft21_K42_42;
shaft21_K40_49 (double)	shaft21_K40_49=shaft21_K42_25;
shaft21_K40_50 (double)	shaft21_K40_50=shaft21_K42_38;
shaft21_K49_28 (double)	shaft21_K49_28=shaft21_K25_41;
shaft21_K49_40 (double)	shaft21_K49_40=shaft21_K25_42;
shaft21_K49_49 (double)	shaft21_K49_49=shaft21_K25_25;
shaft21_K49_50 (double)	shaft21_K49_50=shaft21_K25_38;
shaft21_K50_28 (double)	shaft21_K50_28=shaft21_K38_41;
shaft21_K50_40 (double)	shaft21_K50_40=shaft21_K38_42;
shaft21_K50_49 (double)	shaft21_K50_49=shaft21_K38_25;
shaft21_K50_50 (double)	shaft21_K50_50=shaft21_K38_38;
shaft21_R53_53 (double)	shaft21_R53_53=shaft21_R45_45;
shaft21_R53_54 (double)	shaft21_R53_54=shaft21_R45_46;
shaft21_R53_55 (double)	shaft21_R53_55=shaft21_R45_47;
shaft21_R53_56 (double)	shaft21_R53_56=shaft21_R45_48;
shaft21_R54_53 (double)	shaft21_R54_53=shaft21_R46_45;
shaft21_R54_54 (double)	shaft21_R54_54=shaft21_R46_46;

shaft21_R54_55 (double)	shaft21_R54_55=shaft21_R46_47;
shaft21_R54_56 (double)	shaft21_R54_56=shaft21_R46_48;
shaft21_R55_53 (double)	shaft21_R55_53=shaft21_R47_45;
shaft21_R55_54 (double)	shaft21_R55_54=shaft21_R47_46;
shaft21_R55_55 (double)	shaft21_R55_55=shaft21_R47_47;
shaft21_R55_56 (double)	shaft21_R55_56=shaft21_R47_48;
shaft21_R56_53 (double)	shaft21_R56_53=shaft21_R48_45;
shaft21_R56_54 (double)	shaft21_R56_54=shaft21_R48_46;
shaft21_R56_55 (double)	shaft21_R56_55=shaft21_R48_47;
shaft21_R56_56 (double)	shaft21_R56_56=shaft21_R48_48;
shaft21_TF_yr (double)	
shaft21_Tf_yr2 (double)	
shaft21_R73 (double)	

APPENDIX B

State equation of simulation

Please note: 'd' represents the time derivative of the state variable within the first parenthesis.

$X1=R^{-1}*ID$

d(shaft21_Q50)= X1[11]

d(shaft21_Q49)=SPINNIN1_epcsth*SPINNIN1_SF41+SPINNIN1_P27/SPINNIN1_M27

d(shaft21_Q40)=shaft21_trans36/shaft21_Gyrator2*(shaft21_K38_41*shaft21_Q41+ shaft21_K38_42 *shaft21_Q42 + shaft21_K38_25 * shaft21_Q25 shaft21 _K38_38*shaft21_Q3 - RIGHTEN1_SE3 + shaft21_Fixedto3_cst*X1 [5] + shaft21_Fixedto3_msnt * shaft21_Tf_yr2 *X1[9])

d(shaft21_Q28)= shaft21_trans26*SPINNIN1_P7/SPINNI N1_M7

d(shaft21_Q38)= 1/shaft21_Gyrator2*(RIGHTEN1_SE5- shaft21_trans36*(shaft21 _K40_28 * shaft21_Q28 + shaft21_K40_40 * shaft21_Q40 + shaft21_K40_49 * shaft21_Q49 + shaft21 _ K40 _50 * shaft21 _ Q50) -shaft21 _Fixed to3 _snt* X1[5] -shaft21 _ Fixedto3 _cst * shaft 21 _Tf_yr2*X1[9])

d(shaft21_Q25)= SPINNIN1_P2/SPINNIN1_M2

d(shaft21_Q42)= X1[10]

d(shaft21_Q41)= -SPINNIN1 _ mepsnth *SPINNIN1 _SF41 + SPINNIN1 _P25 / SPINNIN1 _M25

d(shaft21_Fixedto4_Q20)= X1[11]

d(shaft21_Fixedto4_Q19)= X1[10]

d(shaft21_Fixedto4_Q16)= shaft21_Fixedto4_SF15

d(shaft21_Fixedto3_Q20)=1/shaft21_Gyrator2*(shaft21_K38_41*shaft21_Q41+ shaft21 _K38_42*shaft21_Q42 + shaft21_ K38 _25 * shaft21_ Q25 + shaft21

_K38_38*shaft21_Q38- RIGHTEN1_SE3 +shaft21 _ Fixedto3 _ cst *X1[5] +shaft21_Fixedto3_msnt*shaft21_Tf_yr2*X1[9])

d(shaft21_Fixedto3_Q19)=1/shaft21_Gyrator2*(RIGHTEN1_SE5shaft21_trans36 *(shaft21_K40_28*shaft21_Q28 + shaft21 _K40_40 * shaft21_ Q40 +   shaft 21_K40_49*shaft21_Q49+sQ50) -shaft21 _Fixedto3_snt*X1[5]-shaft 21 _ Fixed to3 _ cst *shaft21_Tf_yr2*X1[9])

d(shaft21_Fixedto3_Q16)= shaft21_Fixedto3_SF15

d(shaft21_Fixedto2_Q20)= SPINNIN1_P7/SPINNIN1_M7

d(shaft21_Fixedto2_Q19)= SPINNIN1_P2/SPINNIN1_M2

d(shaft21_Fixedto2_Q16)= shaft21_Fixedto2_SF15

d(shaft21_Fixedto1_Q20)= -SPINNIN1_epcsth *SPINNIN1_SF41 +SPINNIN1 _ P27 /SPINNIN1_M27

d(shaft21_Fixedto1_Q19)= -SPINNIN1 _ mepsnth * SPINNIN1 _ SF41 SPINNIN1 _P25/SPINNIN1_M25 d(shaft21_Fixedto1_Q16)= shaft21 _ Fixedto1_SF15

d(shaft11_Q50)= -SPINNIN1 _ epcsth* SPINNIN1 _ SF41+ SPINNIN1 _ P27 / SPINNIN1_M27

d(shaft11_Q49)= FINITES1_P14/FINITES1_M14

d(shaft11_Q40)= shaft11_trans36*SPINNIN1_P2/SPINNIN1_M2

d(shaft11_Q28)= shaft11_trans26*FINITES1_P12/FINITES1_M12

d(shaft11_Q38)=-SPINNIN1_mepsnth* SPINNIN1 _ SF41 + SPINNIN1 _ P25 / SPINNIN1 _M25

d(shaft11_Q25)= FINITES1_P46/FINITES1_M46

d(shaft11_Q42)= SPINNIN1_P7/SPINNIN1_M7

d(shaft11_Q41)= FINITES1_P44/FINITES1_M44

d(shaft11_Fixedto4_Q20)= -SPINNIN1 _ epcsth* SPINNIN1_ SF41+SPINNIN1_ P27/SPINNIN1_M27

d(shaft11_Fixedto4_Q19)= SPINNIN1_P7/SPINNIN1_M7

d(shaft11_Fixedto4_Q16)= shaft11_Fixedto4_SF15

d(shaft11_Fixedto3_Q20)= SPINNIN1_P2/SPINNIN1_M2

d(shaft11_Fixedto3_Q19)=-SPINNIN1 _mepsnth *SPINNIN1 _SF41 +SPINNIN1_P25/SPINNIN1_M25 d(shaft11_Fixedto3_Q16)= shaft11_Fixedto3_SF15

d(shaft11_Fixedto2_Q20)= FINITES1_P12/FINITES1_M12

d(shaft11_Fixedto2_Q19)= FINITES1_P46/FINITES1_M46

d(shaft11_Fixedto2_Q16)= shaft11_Fixedto2_SF15

d(shaft11_Fixedto1_Q20)= FINITES1_P14/FINITES1_M14

d(shaft11_Fixedto1_Q19)= FINITES1_P44/FINITES1_M44

d(shaft11_Fixedto1_Q16)= shaft11_Fixedto1_SF15

d(SPINNIN1_P2)= -SPINNIN1_pmiomeg*SPINNIN1_P7/SPINNIN1_M7 -SPINNIN1_R4*SPINNIN1_P2/SPINNIN1_M2-shaft11_Gyrator2*(-SPINNIN1_mepsnth*SPINNIN1_SF41+SPINNIN1_P25/SPINNIN1_M25shaft11_trans36*(shaft11_K40_28*shaft11_Q28+shaft11_K40_40*shaft11_Q40+shaft 11 _K40 _49 * shaft11 _Q49 + shaft11 _ K40 _50 * shaft11 _ Q50)-shaft11_Fixedto3_snt*(shaft11_R48_45*(shaft11_Fixedto1_cst*FINITES1_P44/FINITES1_M44+shaft11_Fixedto1_snt*FINITES1_P14/FINITES1_M14+shaft11_Fixedto1_Od1)+shaft11_R48_46*(shaft11_Fixedto2_cst*FINITES1_P46/FINITES1_M46+shaft11_Fixedto2_snt*FINITES1_P12/FINITES1_M12+ shaft11 _Fixed to2 _Od1) + shaft11 _R48_47*(shaft11_Fixedto4_cst*SPINNIN1_P7/SPINNIN1_M7+shaft11_Fixedto4_snt*(-SPINNIN1_epcsth* SPINNIN 1 _SF41 +SPINNIN1 _P27/SPINNIN1_M27) +shaft11 _Fixedto4_Od1) +shaft11_R48_48 *(shaft11_Fixedto3_cst * (SPINNIN1_mepth*SPINNIN1_SF41+SPINNIN1_P25/SPINNIN1_M25)+shaft11_Fixedto3_snt *SPINNIN1_P2/SPINNIN1_M2+shaft11_Fixedto3_Od1))-shaft11_Fixedto3_cst*shaft11_Tf_yr2* (shaft11 _R56 _53 *shaft11 TF_yr * (shaft11 _Fixed to2_msnt*FINITES1_P46/FINITES1_M46+ shaft11 _Fixedto 2 _cst* FINITES1_P12/FINITES1_M12+shaft11_Fixedto2_Od2)+shaft11_R56_54*(shaft11_Fixedto1_msnt*FINITES1_P44/FINITES1_M44+shaft11_Fixedto1_cst*FINITES1_P14/FINITES1_M14+shaft11_Fixedto1_Od2)+shaft11_R56_55*(shaft11_Fi

xedto4_msnt*SPINNIN1_P7/SPINNIN1_M7+shaft11_Fixedto4_cst*(SPINNIN1_epcsth*SPINNIN1_SF41+SPINNIN1_P27/SPINNIN1_M27)+shaft11_Fixedto4_Od2)+shaft11_R56_56*shaft11_Tf_yr2*(shaft11_Fixedto3_msnt*(SPINNIN1_mepsnth*SPINNIN1_SF41+SPINNIN1_P25/SPINNIN1_M25)+shaft11_Fixedto3_cst*SPINNIN1_P2/SPINNIN1_M2+shaft11_Fixedto3_Od2))-shaft21_K25_41*shaft21_Q41-shaft21   _K25   _42*shaft21_Q42-shaft21_K25_25*shaft21_Q25-shaft21_K25_38* shaft21 _Q38 +shaft21 _Gyrator1 *SPINNIN1 _P7/SPINNIN1 _M7 -shaft 21 _Fixedto2_cst* X1[3]shaft21 _Fixedto2 _msnt * shaft21 _TF _ yr *X1[6]

d(SPINNIN1_P25)= -SPINNIN1_R11*(- SPINNIN1_ mepsnth*SPINNIN1_ SF41 +SPINNIN1_P25/SPINNIN1_M25)-shaft11 _K38_41 * shaft11 _ Q41 −shaft 11_K38_42*shaft11_Q42-shaft11_K38_25*shaft11_Q25 -shaft 11 _K38 _ 38 * shaft   11_Q38+shaft11_Gyrator2*SPINNIN1_P2/SPINNIN1_M2-shaft   11_ _cst*(shaft11_R48_45*(shaft11_Fixedto1_cst*FINITES1_P44/FINITES1_M44+shaft11_Fixedto1_snt*FINITES1_P14/FINITES1_M14+shaft11_Fixedto1_Od1)+shaft11_R48_46*(shaft11_Fixedto2_cst*FINITES1_P46/FINITES1_M46+shaft11_Fixedto2_snt*FINITES1_P12/FINITES1_M12+shaft11_Fixedto2_Od1)+shaft11_R48_47*(shaft11_Fixedto4_cst*SPINNIN1_P7/SPINNIN1_M7+shaft11_Fixedto4_snt*(-SPINNIN1_epcsth*SPINNIN1_SF41+SPINNIN1_P27 /SPINNIN1_M27) +shaft11_Fixedto4_Od1)+shaft11_R48_48*(shaft11_Fixedto3_SPINNIN1_mepsnth*SPINNIN1_SF41+SPINNIN1_P25/SPINNIN1_M25)+shaft11_Fixedto3_snt *SPINNIN1_P2/SPINNIN1_M2+shaft11_Fixedto3_Od1))-shaft11_Fixedto3   _ msnt*shaft11_Tf_yr2*(shaft11_R56_53*shaft11_TF_yr*(shaft11_Fixedto2_msnt*FINITES1_P46/FINITES1_M46+shaft11_Fixedto2_cst*FINITES1_P12/FINITES 1_M12+shaft11_Fixedto2_Od2)+shaft11_R56_54(shaft11_Fixedto1_msnt*FINITES1_P44/FINITES1_M44+shaft11_Fixedto1_cst*FINITES1_P14/FINITES1_M1 4+shaft11_Fixedto1_Od2)+shaft11_R56_55*(shaft11_Fixedto4_msnt *SPINNIN1_P7/SPINNIN1_M7+shaft11_Fixedto4_cst*(-SPINNIN1   _epcsth *SPINNIN1_SF41+SPINNIN1_P27/SPINNIN1_M27)+shaft11_Fixedto4_Od2)+s haft11_R56_56*shaft11_Tf_yr2 *(shaft11_Fixedto3_msnt*(-SPINNIN1 _mepsnth *SPINNIN1_SF41+SPINNIN1_P25/SPINNIN1_M25)+shaft11_Fixedto3_cst*SPI NNIN1_P2/SPINNIN1_M2+shaft11_Fixedto3_Od2))-shaft21 _K41_41 *shaft21 _Q41 -shaft21_K41_42*shaft21_Q42-shaft21 _K41_25 *shaft21   _Q25-shaft21

$\_K41\_38$ *shaft21_Q38-shaft21_Fixedto1_cst*X1[2]-shaft21 _Fixed to 1_msnt * X1[7]-shaft21_R73 *(-SPINNIN 1_mepsnth *SPINNIN1 _SF41 +SPINNIN1 _P25/SPINNIN1_M25)

d(SPINNIN1_Q28)= SPINNIN1_P27/SPINNIN1_M27

d(SPINNIN1_Q26)= SPINNIN1_P25/SPINNIN1_M25

d(SPINNIN1_Q3)= SPINNIN1_P2/SPINNIN1_M2

d(SPINNIN1_Q8)= SPINNIN1_P7/SPINNIN1_M7

d(SPINNIN1_Q24)= SPINNIN1_SF41

d(BEARING2_P8)= -BEARING2_K13*BEARING2_Q13-BEARING2 _R14 * (BEARING2 _P8/BEARING2_M8-SF74)-RIGHTEN1_SE18 +X1[1]

d(BEARING2_P1)= -RIGHTEN1_SE15+X1[0]-BEARING2 _K6 *BEARING2 _ Q6-BEARING2_R7*(BEARING2_P1/BEARING2_M1-SF73)

d(BEARING2_Q13)= BEARING2_P8/BEARING2_M8-SF74

d(BEARING2_Q6)= BEARING2_P1/BEARING2_M1-SF73

d(FINITES1_Q30)= FINITES1_P14/FINITES1_M14-BEARING1 _ P8 / BEARING1_M8

d(FINITES1_Q38)= FINITES1_P34/FINITES1_M34-BEARING 1 _ P8 / BEARING _M8

d(FINITES1_Q4)=1/FINITES1_mmu*(1/FINITES1_Munit*FINITES1_P14/FINITES1_M14-1/FINITES1_Munit *FINITES1_P34/FINITES1_M34)

d(FINITES1_Q3)= 1/FINITES1_mu*(FINITES1_P12/FINITES1_M12-FINITES1_P32/FINITES1_M32)

d(FINITES1_Q28)= FINITES1_P12/FINITES1_M12-BEARING 1_ P1 BEARING 1_M1

d(FINITES1_Q36)= FINITES1_P32/FINITES1_M32-BEARING 1_ P1 / BEARING1_M1

d(BEARING1_P8)= -BEARING1_K13*BEARING1_Q13- BEARING1 _R14 * (BEARING1 _P8/BEARING1_M8-SF68)+FINITES1_K38 * FINITES1 _Q38 + FINITES1_R242*(FINITES1_P34/FINITES1_M34- BEARING 1 _P8 / BEARING1_M8) +FINITES1_R240*(FINITES1_P14/FINITES1_M14- BEARING1_P8/BEARING1_M8)+FINITES1_K30*FINITES1_Q30

d(BEARING1_Q13)= BEARING1_P8/BEARING1_M8-SF68

d(BEARING1_Q6)= BEARING1_P1/BEARING1_M1-SF67

d(RIGHTEN1_Q16)= X1[11]-BEARING2_P8/BEARING2_M8

d(RIGHTEN1_Q13)= X1[10]-BEARING2_P1/BEARING2_M1